Acta Oceanol. Sin., 2022, Vol. 41, No. 1, P. 99–117
https://doi.org/10.1007/s13131-021-1865-4
http://www.aosocean.com
E-mail: ocean2@hyxb.org.cn

Environmental drivers of phytoplankton crops and taxonomic composition in northeastern Antarctic Peninsula adjacent sea area

Yubin Feng[1], Dong Li[1]*, Jun Zhao[1], Zhengbing Han[1], Jianming Pan[1], Gaojing Fan[1], Haisheng Zhang[1], Ji Hu[1], Haifeng Zhang[1], Jiaqi Wu[1], Qiuhong Zhu[1]

[1] Key Laboratory of Marine Ecosystem Dynamics, Second Institute of Oceanography, Ministry of Natural Resources, Hangzhou 310012, China

Received 1 April 2021; accepted 7 June 2021

Abstract

The ecosystem of the sea region adjacent to the Antarctic Peninsula is undergoing remarkable physical and biological changes, in the context of global warming. However, understanding of the dynamics of phytoplankton taxonomic composition in this marginal ice zone remains unclear. In this study, seawater samples collected from 36 stations in the northeastern Antarctic Peninsula were analyzed for nutrients and phytoplankton pigments. Combining with CHEMTAX analysis, remote sensing data, and physicochemical measurements, we investigated the relationships between phytoplankton crops, taxonomic composition, and marine environmental drivers. Integrated chlorophyll *a* (Chl *a*) concentrations (200 m) varied from 8.9 mg/m^2 to 64.2 mg/m^2, with an average of (23.2±12.0) mg/m^2 and higher phytoplankton biomass concentrated in the coastal region of South Orkney Island and South Shetland Island. Diatoms were the dominant functional group (63%±21%). Higher proportions of diatoms were associated with higher Chl *a* (r=0.40, p<0.01), stable water columns (r=0.20, p<0.01), higher Si/P ratios (r=0.34, p<0.01), higher photosynthetically active radiation intensity (r=0.64, p<0.01), and higher sea ice melt water contributions (MWC, r=0.20, p<0.01). Conversely, *Phaeocystis antarctica* contributed a smaller overall proportion (31%±18%) and was more concentrated in the offshore water masses (e.g., Philip Ridge and South Scotia Ridge) with lower light levels (r=–0.58, p<0.01), deeper mixed layer depths (r=0.17, p<0.05), higher nutrient concentrations (e.g., N, P, and Si, r>0.35, p<0.01), and lower MWC (r=–0.20, p<0.01). In comparison, the total contribution from green flagellates (4%±5%), cryptophyta (1%±3%), dinoflagellates (1%±4%), and cyanobacteria (1% ± 5%) was only 6%. In offshore regions with well-mixed water, less varied taxonomic composition and lower crops with a higher proportion of nanophytoplankton were observed. In contrast, significantly decreasing crops below the mixed layer depth was observed in water columns with strong stratification, where the dominant phytoplankter changed from diatoms to *P. antarctica*. These findings have important implications for better understanding the future dynamics of marine ecosystems in the sea area adjacent to the Antarctic Peninsula.

Key words: Antarctic Peninsula, phytoplankton crops, phytoplankton taxonomic composition, pigment, light intensity, mixed layer depth

Citation: Feng Yubin, Li Dong, Zhao Jun, Han Zhengbing, Pan Jianming, Fan Gaojing, Zhang Haisheng, Hu Ji, Zhang Haifeng, Wu Jiaqi, Zhu Qiuhong. 2022. Environmental drivers of phytoplankton crops and taxonomic composition in northeastern Antarctic Peninsula adjacent sea area. Acta Oceanologica Sinica, 41(1): 99–117, doi: 10.1007/s13131-021-1865-4

1 Introduction

The ocean is an important carbon dioxide sink and plays key roles in buffering rising atmospheric carbon dioxide (CO_2) and climate change (Landschützer et al., 2016). Although the Southern Ocean (south of 50°S) accounts for only 10% of the ocean area, based on the efficient biological pump and solubility pump, it could account for 25% of the CO_2 consumption of the global ocean (Takahashi et al., 2002). Thus, the Southern Ocean acts as an important response and regulation area for global ocean carbon cycling (Sabine et al., 2004; Steig et al., 2009). In particular, due to its hydrological and trophic conditions (e.g., nutrients, light, and temperature) (Cheah et al., 2017; Deppeler and Davidson, 2017; Lee et al., 2016), the seasonal marginal ice zone distributed around the Antarctic continent is a highly productive region (Petrou et al., 2016) and supports massive biomass (Loeb et al., 2010; Pallin et al., 2018).

Phytoplankton serve as the major producer and food source for the entire marine ecosystem (Schloss et al., 2012). Different functional groups of the phytoplankton play distinct roles in marine primary productivity (Deppeler and Davidson, 2017), food-web stability (Forcada et al., 2012), marine biological resource biomass (Loeb et al., 2010), and the biological pump efficiency (Kerr et al., 2018a; Tréguer et al., 2018). Moreover, the Antarctic Ocean is one of the largest ecosystems on Earth, with a unique and very short food chain (i.e., Diatom–Krill–Top predator) and a huge amount of biological resources. This simple food chain and

Foundation item: The program of Impact and Response of Antarctic Seas to Climate Change under contract No. IRASCC2020-2022 (01-01-02 and 02-02); the National Natural Science Foundation of China under contract Nos 41976228, 41976227 and 41506223; the Scientific Research Fund of the Second Institute of Oceanography under contract Nos JG1805, JG2011 and JG2013.
*Corresponding author, E-mail: lidong@sio.org.cn

limited biodiversity make the Antarctic Ocean sensitive to environmental change (Forcada et al., 2012; Kerr et al., 2018b). Previous studies have reported that climate-driven ice–sea interactions in Antarctica have accelerated the melting of ice shelves, leading to a series of environmental changes in the upper layers of the water column, such as decreased salinity, dissolved Fe input (Costa et al., 2020; Mendes et al., 2018b) and water column mixing (Peck et al., 2010; Stammerjohn et al., 2008). However, how this changing environmental drivers affect phytoplankton crops and community structure in key areas of the Antarctic Ocean is not clear yet, as there are currently scarce resources on this subject (Kerr et al., 2018b). Thus, to maintain the stability of the marine ecosystem and resources in the Antarctic Ocean, it is necessary to study the mechanism of ecological dynamics and key environmental factors.

The northern Antarctic Peninsula is a transition environment with sub-polar to polar influence (Rodriguez et al., 2002). It is considered to be a marine climate hotspot for rapid changes in sea ice (variations in glacier size, seasonal sea ice extent, and thickness of ice shelf), ocean (deep water cooling, freshening and lightening, and surface warming), and ecosystem dynamics (phytoplankton composition changes and krill and salp density) (Kerr et al., 2018b; Shepherd et al., 2018; Stammerjohn et al., 2008). The study area generally showed microelement deficiency (e.g., Fe) characteristics during summer (Wang et al., 2020), and Fe inputs sourced from meteoric and glacial meltwater may relieve the Fe limitation of the coastal region during the ice-melting season. Biologically, the Antarctic Peninsula serves as an important spawning ground for krill (Loeb et al., 2010) and whales (Secchi et al., 2011). Through regulating the hydrodynamic conditions and trophic status of seawater (Kerr et al., 2018b; Seyboth et al., 2018), the changes in the regional climate and sea ice dynamics could affect all trophic level organisms (from microbes, primary producers, zooplanktonic organisms, and fish to predators) despite different degrees of affinity to the sea ice (Ducklow et al., 2012). Furthermore, previous studies documented that the food chain and composition of the phytoplankton community are changing much more frequently (even annually) in some regions of the western Antarctica Peninsula (Garibotti et al., 2005; Mendes et al., 2013). Hence, tracking the spatial and temporal changes of phytoplankton crops and taxonomic composition in this highly productive region is of great significance for understanding the regional ecological response of the Southern Ocean in the context of climate change (Mendes et al., 2012, 2013, 2018a). Many studies have focused on the near-shore waters around the western Antarctic Peninsula (Clarke et al., 2007; Garibotti et al., 2005; Kozlowski et al., 2011; Montes-Hugo et al., 2009). However, due to the lack of continuous monitoring programs and scarcity of fundamental studies (Kerr et al., 2018b; Sanchez et al., 2019; Wang et al., 2020), there are needs to perform surveys with broader spatial and finer temporal scale in phytoplankton dynamics (i.e., crops and composition) of the northern and eastern Antarctic Peninsula sea area.

To probe the main drivers controlling the spatial dynamics of phytoplankton crops and taxonomic composition within the coastal region of the northeastern Antarctic Peninsula, water samples from 36 stations were collected. The *in situ* hydrological data (i.e., salinity, potential temperature, and potential density), macro-nutrients, and remote sensing data (e.g., photosynthetically active radiation (PAR)) were obtained to study the spatial distribution of environmental factors. Phytoplankton pigments were analyzed and the chemical taxonomy (CHEMTAX) method based on pigment composition was applied to carefully examine the phytoplankton crops and phytoplankton taxonomic composition for the entire area. This study thus provides insight into the spatial variability of phytoplankton crops and taxonomic composition in this fast-changing region, and sheds new light on the evolving trends of the phytoplankton community and food webs in the Antarctic Ocean under climate change.

2 Material and methods

2.1 *Field sampling and oceanographic measurements*

Thirty-six stations were sampled from the R/V *Xuelong* as a part of the 32nd Chinese National Antarctica Research Expedition (CHINARE) in the north tip of the Antarctic Peninsula, from 59°S to 64°S and from 43°W to 61°W, during the early summer from December 19, 2015 to January 14, 2016 (Fig. 1). Hydrologic-

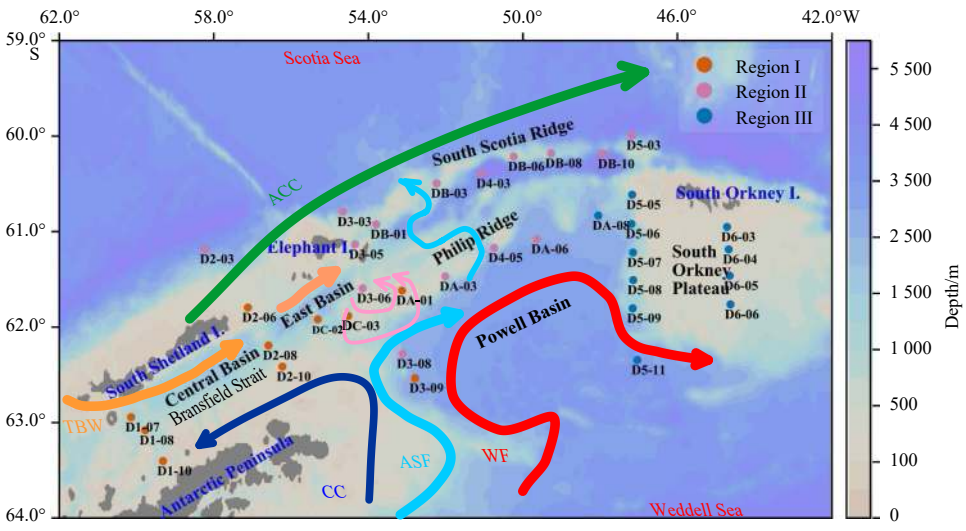

Fig. 1. Study sites, ocean currents, and sampling locations during 2015–2016 summer cruises. Transitional Bellingshausen Water (TBW, orange arrow), coastal current (CC, blue arrow), Antarctic Slope Front (ASF, light blue arrows), Weddell Front (WF, red arrow), Antarctic Circumpolar Current (ACC, green arrow) and anticyclonic eddy (pink arrows) are indicated by different colored arrows (Sanchez et al., 2019; Thompson et al., 2009).

al data (including temperature, salinity, and density) were measured by Sea-Bird SBE-9/11 plus CTD (conductivity-temperature-depth system, Bellevue, U.S.A.), which was pre-calibrated (Fig. 2a). Water samples were taken from five layers at 0 m, 25 m, 50 m, 100 m, and 200 m for phytoplankton pigment analysis and nutrient analysis.

2.2 *Nutrient analysis*

Seawater samples were filtered through pre-washed cellulose acetate membrane filters (0.45 μm) to determine dissolved inorganic nutrients (nitrate, phosphate, and silicate). Filtered water samples were stored at –20°C until further analysis. Nutrients were analyzed using a continuous flow analyzer (Skalar Analytic-

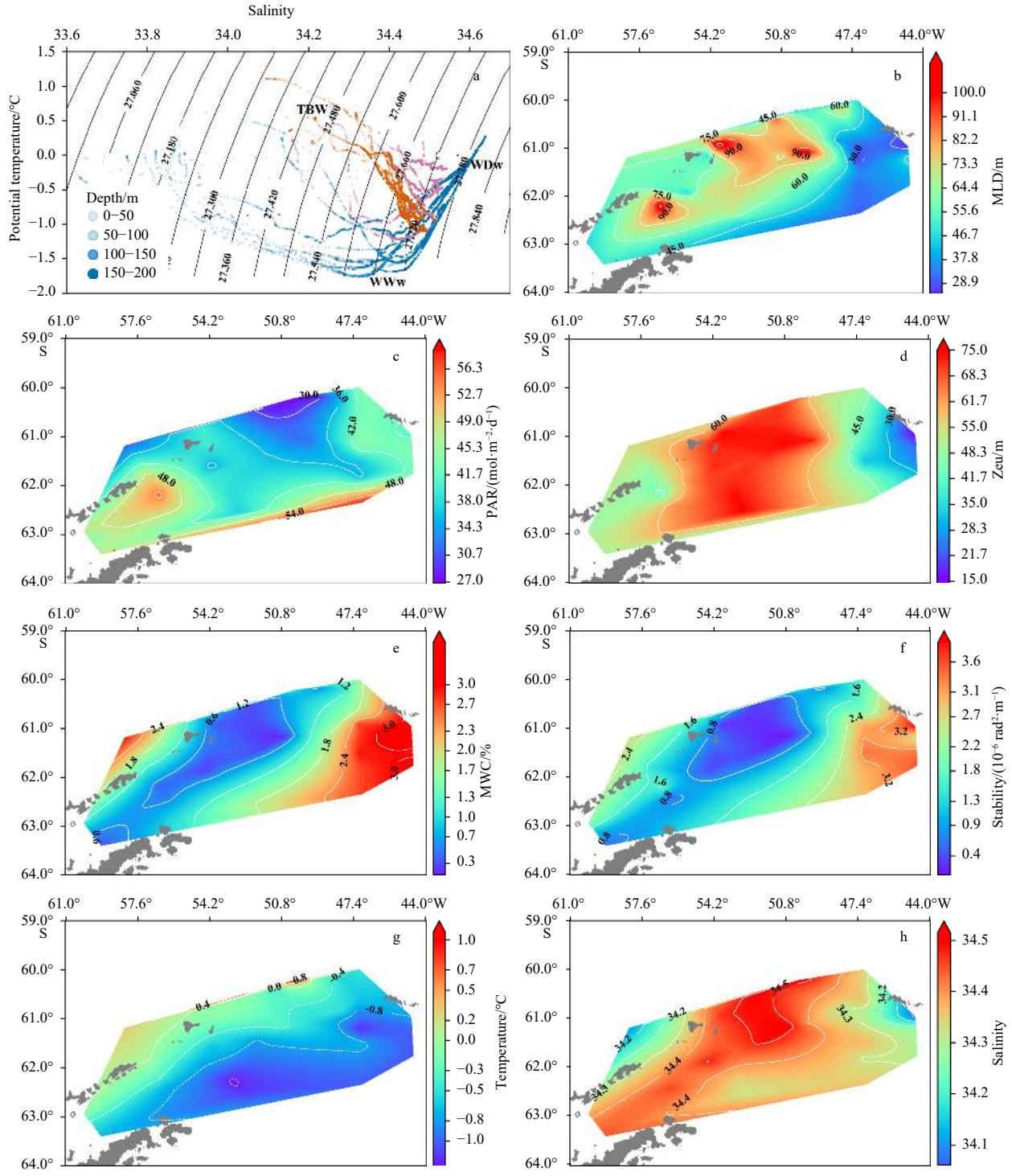

Fig. 2. Oceanographic and hydrological characteristics of the study area. The *T-S* diagram of the study area (0–200 m) (a) (Region I: orange dots, Region II: pink dots, and Region III: blue dots, gray curve were contours of potential density σ (kg/m³)); TBW, Transitional Bellingshausen Water; WDw, Weddell Sea deep water; WWw, Weddell Sea winter water. Distributions of the mixed layer depth (MLD) (b), photosynthetically active radiation (PAR) (c), euphotic layer depth (Zeu) (d), meltwater contribution percentage (MWC) (e), water column stability (f), temperature (g) and salinity (h).

al, Breda, Netherlands) following a method reported by Grasshoff et al. (1999). The detection limits were 0.1 μmol/L for nitrate, 0.1 μmol/L for silicate, and 0.03 μmol/L for phosphate.

2.3 *UPLC pigment analysis and CHEMTAX analysis*

For pigment samples, 3 L of seawater was filtered using GF/F glass fiber filter (Whatman, New Castle, U.S.A.) under gentle vacuum (<0.5 atm) and dim light conditions, and then stored at –80°C until lab analysis. Prior to instrumental analysis, samples were pre-treated according to the method described in Zapata et al. (2000). The pigments were extracted with 3 mL of acetone, ultrasonicated in an ice bath for 30 s, and then stored at –20°C for 2 h. The extract was separated from filter debris, and the supernatant was dried under gentle N_2 stream and re-dissolved with a 300 μL mixture of methanol and water (9:1, V/V). The analysis was completed within 4 h. Pigment extracts were analyzed using Acquity H-Class Ultra Performance Liquid Chromatography (UPLC, Waters Corp., Milford, U.S.A.) comprising UPLC-Quaternary Solvent Manager, Sample Manager-FTN, PDAeλ Detector, and FLR Detector. The analysis used the Acquity UPLC® BEH C18 Column (50 mm long, 2.1 mm in diameter, and 1.7 μm particle size) at a flow rate of 0.4 mL/min. A binary gradient elution program was used according to Zapata et al. (2000) (Table S1). Pigments were qualitatively and quantitatively detected by comparing retention time, absorption spectra, and area of the peaks in each sample chromatogram with those of authentic standards purchased from DHI Water and Environment (Hørsholm, Denmark) (Table S2, Fig. S1). Pigment standards used in this study were chlorophyll *a* (Chl *a*), chlorophyll *b* (Chl *b*), chlorophyll c_3 (Chl c_3), chlorophyll c_2 (Chl c_2), pheophytin *a* (Phytin-*a*), pheophobide *a* (Phide-*a*), alloxanthin (Allo), 19´-butanoyloxyfucoxanthin (But-fuco), fucoxanthin (Fuco), 19'-hexanoyloxyfucoxanthin (Hex-fuco), peridinin (Peri) and zeaxanthin (Zea), respectively. The precision and detection limits of the method were 0. 26 μg/L and 2.2 μg/L, respectively.

The CHEMTAX program (Version 1.95), proposed by Wright et al. (2009), used ten diagnostic pigments (Table 1) to differentiate the relative contributions of six major taxonomic groups to total Chl *a* biomass. It is assumed that different algae contain specific pigments and a defined proportion of pigment concentration (based on Chl *a*) in the study area (Garibotti et al., 2003; Mendes et al., 2012, 2013; Russo et al., 2018). For example, Chl c_3 and Chl *b* are the diagnostic pigments of *Phaeocystis antarctica* (*P. antarctica*) and green flagellates (with Chl *b*), respectively. The green flagellates evaluated in this CHEMTAX analysis are not assigned to a distinct algal group, but referred as flagellates (e.g., *Chlorophyceae*, *Prasinophyceae*, and *Pyramimonas*) bearing Chl *b* (Peeken, 1997; Rodriguez et al., 2002; Mendes et al., 2012, 2013, 2018b; Russo et al., 2018). Previous studies have pointed out these green algae may originate from sea-ice and could survive under unfavourable seawater environments (Peeken, 1997). Moreover, Chl c_2 and Fuco are found in both diatoms and *P. antarctica*., Allo, Peri, and Zea are the diagnostic pigments of the cryptophyta, dinoflagellates, and cyanobacteria, respectively. Comparing with optical microscopy observation, this CHEMTAX model has been successfully applied in characterizing phytoplankton assemblages in the Antarctic coastal waters (Rodriguez et al., 2002; Garibotti et al., 2003; Mendes et al., 2012, 2013; Van de Poll et al., 2011; Costa et al., 2020).

Based on our pigment data and the initial matrix of the literature, we identified six algae and pigment-algae initial matrices that may be present in the region (Table 1). The pigment-algae matrix is affected by environmental factors such as irradiance and nutrients (Barlow et al., 2008), so there is often a gap between the initial matrix and the actual value of the study area. CHEMTAX continually modifies the initial matrix by factor analysis and steepest descent algorithms, reducing the size of the residuals to make the matrix closer to the true value. To prevent the algorithm from identifying the local minimum as the result, we created 60 random starts based on the initial matrix. If they ob-

Table 1. Ratios of concentrations of diagnostic pigment to chlorophyll *a* (Chl *a*) used for CHEMTAX analysis (Wright et al., 2009). Zeaxanthin (Zea), chlorophyll c_3 (Chl c_3), chlorophyll c_2 (Chl c_2); peridinin (Peri), 19'-butanoyloxyfucoxanthin (But-fuco), fucoxanthin (Fuco), 19'-hexanoyloxyfucoxanthin (Hex-fuco), alloxanthin (Allo), chlorophyll *b* (Chl *b*), and Chl *a* are used in calculations

	Zea	Chl c_3	Chl c_2	Peri	But-fuco	Fuco	Hex-fuco	Allo	Chl *b*	Chl *a*
Input matrix (initial ratios before analysis)										
Diatoms	0	0	0.110	0	0	0.754	0	0	0	1
Dinoflagellates	0	0	0.320	0.720	0	0	0	0	0	1
Cyanobacteria	0.190	0	0	0	0	0	0	0	0	1
P. antarctica	0	0.141	0.144	0	0.080	0.011	0.916	0	0	1
Cryptophytes	0	0	0.174	0	0	0	0	0.228	0	1
Green flagellates	0.030	0	0		0	0	0	0	0.945	1
Output matrix (optimized ratios for 0–50 m bin)										
Diatoms	0	0	0.247	0	0	1.593	0	0	0	1
Dinoflagellates	0	0	0.330	1.071	0	0	0	0	0	1
Cyanobacteria	0.178	0	0	0	0	0	0	0	0	1
P. antarctica	0	0.429	0.102	0	0.146	0.021	0.969	0	0	1
Cryptophytes	0	0	0.148	0	0	0	0	0.312	0	1
Green flagellates	0	0	0	0	0	0	0	0	1.382	1
Output matrix (optimized ratios for 100–200 m bin)										
Diatoms	0	0	0.317	0	0	1.427	0	0	0	1
Dinoflagellates	0	0	0.251	0.362	0	0	0	0	0	1
Cyanobacteria	0.252	0	0	0	0	0	0	0	0	1
P. antarctica	0	0.296	0.120	0	0.134	0.014	0.774	0	0	1
Cryptophytes	0	0	0.211	0	0	0	0	0.254	0	1
Green flagellates	0	0	0	0	0	0	0	0	0.857	1

tained the same result, we concluded that the final matrix was the real pigment-algae matrix of the study area, and the run result was the real phytoplankton taxonomic composition of the study area. To account for the variation of pigment ratios with irradiance and/or nutrient availability, data were also split into two bins according to sample depth (0–50 m and 100–200 m).

2.4 *Integrated water column values*

To overcome the statistical error caused by the analysis of non-equal sampling depth, this study used water column integral pigment concentration (Zhuang et al., 2014) to evaluate the regional distribution of diagnostic pigments and the Chl *a* degradation product. The integrated values were calculated as

$$C_{\text{int}} = [C_1 (D_1 + D_2) + C_2 (D_3 - D_1) + \cdots + C_n (D_n - D_{n-1})]/2, \quad (1)$$

where D_n was the measured depth at a layer and C_n was the concentration at this layer.

2.5 *Remote sensing data and physical measurements of marine environmental factors*

The PAR and euphotic layer depth (Zeu) measured by remote sensing during our sampling time (8 d averaged) were downloaded from SeaWiFs (http://oceancolor.gsfc.nasa.gov/DOCS/seawifs_par_wfigs.pdf) and Morel et al. (2007). Data within 30 km×30 km of the observation stations were selected for evaluation.

To evaluate the influence of fresh water, the meltwater percentage (MWC) was calculated as the difference of salinity between surface water (S_{surface}) and deep water (S_{deep}, around 300 m) at the same station, according to the method reported by Mendes et al. (2018b), and Costa et al. (2020). The calculating equation is shown as below:

$$\text{MWC} = \left(1 - \frac{S_{\text{surface}} - 6}{S_{\text{deep}} - 6}\right) \times 100, \quad (2)$$

where in the S_{deep} was assumed not to be influenced by sea ice dilution and the salinity of sea ice was set as 6 (Ackley et al., 1979).

The potential density of seawater (ρ, kg/m^3) was determined by the potential temperature, salinity, and pressure data. The mixed layer depth (MLD) was calculated by finding the depth of the maximum water column buoyancy frequency, max (N^2, rad^2/s^2) (Carvalho et al., 2016), which is determined by

$$N^2 = \frac{g}{\rho}\frac{\partial \rho}{\partial z}, \quad (3)$$

where g is gravity, z is the water depth. The stability of the water column ($E_{\text{stability}}$, 10^{-6} rad^2/m) was further estimated according to Eq. (4):

$$E_{\text{stability}} = \frac{N^2}{g}. \quad (4)$$

The average values of $E_{\text{stability}}$ between 0 to 100 m depth were used in this study to represent the horizontal variation of the water column stability at each station (Costa et al., 2020; Mendes et al., 2018b).

2.6 *Statistical analysis*

Relationships between relative abundance of phytoplankton groups and environmental variables at the surface were explored by redundancy analysis (RDA) using the "vegan" package (Oksanen et al., 2013) in the program R. The variables used in the RDA included the percent of CHEMTAX-derived taxonomical groups to whole phytoplankton crops, PAR, MLD, sea surface temperature, sea surface salinity (salinity), MWC, $E_{\text{stability}}$, dissolved inorganic nitrogen (DIN; including nitrate, nitrite, and ammonium), phosphate, and silicate. Monte-Carlo tests were run in order to evaluate the significance of the RDA. Significant differences between treatments were tested using a one-way analysis of variance (ANOVA) (α=0.05). Pearson linear correlations between study parameters were calculated using SPSS.

3 Results

To investigate the environmental factors regulating phytoplankton taxonomic groups, the study area was clustered into three regions from west to east according to the *k*-means clustering of CHEMTAX-derived phytoplankton taxonomic composition (Fig. 1). Region I is an area surrounded by islands (e.g., the tip of Antarctic Peninsula, South Shetland Island, and Elephant Island). Region II is a more open sea area dominated by ridges (e.g., South Scotia Ridge and Philip Ridge) and a deep basin (Powell Basin). Region III mainly lies south of the South Orkney Island and upon the South Orkney Plateau.

3.1 *Environmental setting*

The environmental settings in the study area differ dramatically. For instance, Region III has the shallowest MLD [(36±7) m] and lowest water temperature [(−0.67±0.70)°C] and salinity (34.2±0.3) compared with Region I [(63±20) m, (−0.37±0.56)°C, 34.4±0.1] and Region II [(70±20) m, (−0.15±0.63)°C, 34.4±0.2] (p<0.05) (Table2). Correspondingly, Region III contributed 3–4 times more sea ice melt water (MWC, 2.8%±0.6%) and had the strongest stability of water column (3.0±0.6) compared with Re-

Table 2. Average (±standard deviation), minimum and maximum (in parenthesis) values of environmental parameters for each sampling region (Regions I, II and III)

	Region I (n=50)	Region II (n=75)	Region III (n=54)
Temperature/°C	−0.37±0.56 (−1.45–1.06)	−0.15±0.63 (−1.6–1.65)	−0.67±0.69 (−1.7–0.5)
Salinity	34.39±0.10 (34.12–34.52)	34.39±0.16 (33.82–34.65)	34.19±0.28 (33.59–34.63)
MLD/m	63.1±19.51 (45–107)	70.2±19.83 (39–111)	35.56±6.84 (25–49)
Meltwater proportion/%	0.68±0.45 (0.26–1.67)	0.87±0.70 (0.15–2.94)	2.75±0.54 (1.67–3.62)
Stability/(10^{-6} rad^2·m^{-1})	1.08±0.58 (0.4–2.15)	0.93±0.69 (0.12–2.72)	3.00±0.54 (1.91–3.91)
Phosphate concentration/(μmol·L^{-1})	2.07±0.15 (1.53–2.29)	2.17±0.13 (1.83–2.44)	2.00±0.38 (0.81–2.6)
Silicate concentration/(μmol·L^{-1})	85.73±5.21 (74.03–95.34)	85.59±7.01 (69.24–100.6)	85.49±9.49 (69.09–111.16)
Nitrate concentration/(μmol·L^{-1})	28.26±3.29 (21.42–36.8)	29.78±2.51 (22.88–34.02)	26.88±5.66 (7.04–36.65)
Chl *a*/(μg·L^{-1})	0.17±0.18 (0–0.72)	0.12±0.07 (0–0.3)	0.13±0.13 (0–0.68)

gion I (0.7%±0.4%, 1.1±0.6) and Region II (0.9%±0.7%, 0.9±0.7). Additionally, based on the remote sensing data, the calculated average PAR (during the past month before sampling) was higher in Region I [(46±6) mol/(m²·d)] and Region III [(43±6) mol/(m²·d)], with a significantly lower value in Region II [(34±5) mol/(m²·d)]. The estimated Zeu was shallowest in Region III [(36±12) m], with deeper values in Region I [(58±11) m] and Region II [(66±10) m] (Fig. 3). Additionally, MLD was deeper in the basin and ridge re-

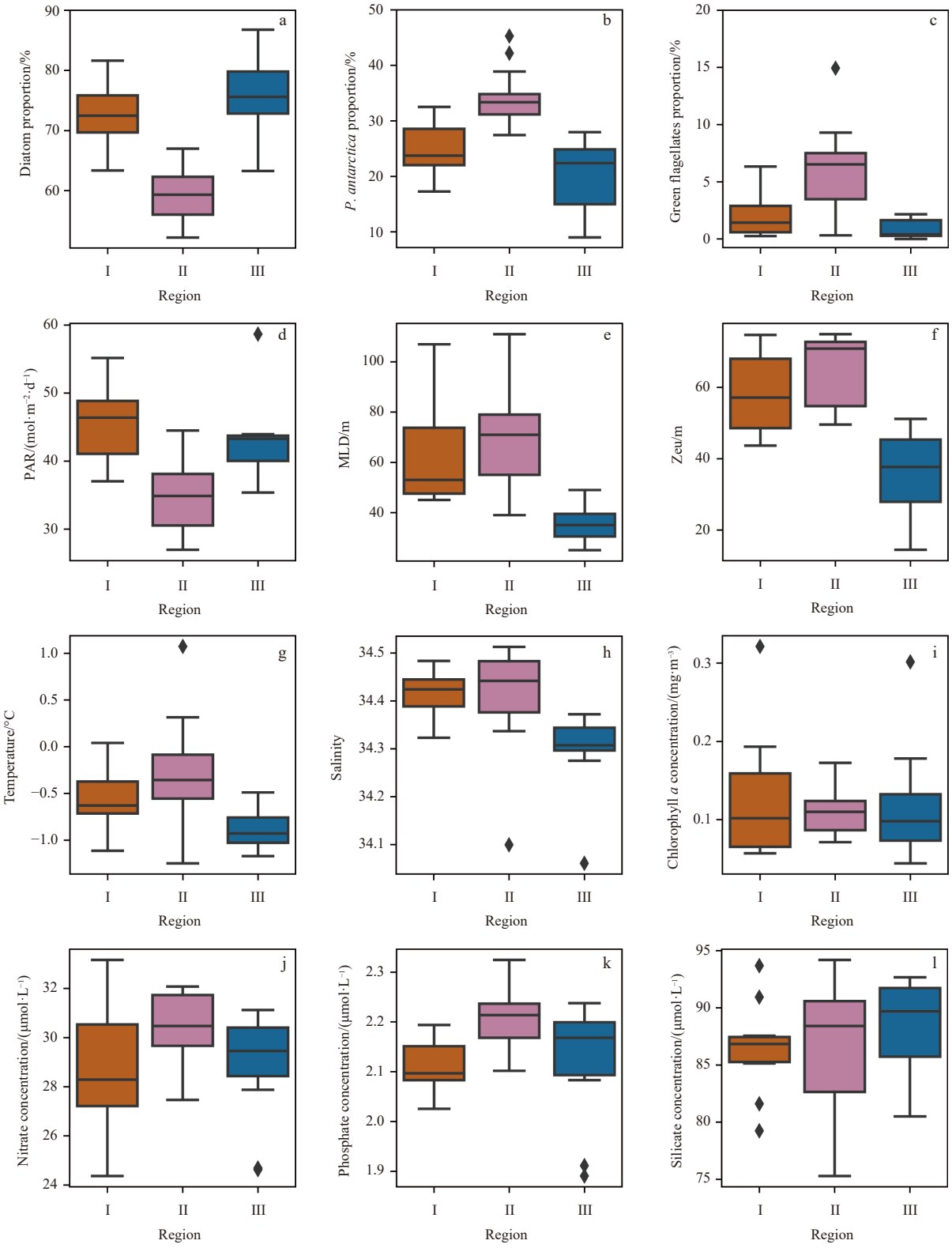

Fig. 3. Boxplots of phytoplankton taxonomic composition (only the most abundant three groups were shown) and environmental factors in Region I (orange), Region II (pink) and Region III (blue). The horizontal lines of the boxes represent 25%, 50% (median), and 75% percentiles (from bottom to top). Dots indicate extreme values (outliers).

gion and shallower in the South Orkney Plateau region (Fig. 2b). The area with high values of salinity and temperature changed from mostly concentrated in the upper layers of Regions I and II to lower layers of Region III (Fig. S2). Water temperature generally decreased with greater water depth (p<0.01), with a warm water mass upwelling in the 200 m layer of Region III. The salinity generally showed an increasing trend with increasing water depth (p<0.01, Fig. S1b). Generally, the physical characteristics of the three regions differed significantly, with maximum density variation in Region III and minimum variation in Region II (Fig. 2a). The distribution of Zeu was similar with MLD, and the average of Zeu was (54±16) m. The Zeu in Region III was lower than in Region I (Fig. 2d).

3.2 *Nutrient concentrations and ratios*

In this study, the silicate concentration ranged from 69.1 μmol/L to 111.2 μmol/L [mean: (85.6±7.6) μmol/L], the nitrate concentration ranged from 7.0 μmol/L to 36.8 μmol/L [(28.5±4.1) μmol/L], and the phosphate concentration ranged from 0.8 μmol/L to 2.6 μmol/L [mean: (2.1±0.3) μmol/L]. Regionally, significantly higher phosphate [(2.2±0.1) μmol/L] and nitrate [(29.8±2.5) μmol/L] were observed in Region II, and no significant differences existed between Region I [(2.1±0.2) μmol/L, (28.3±3.3) μmol/L] and III [(2.0±0.4) μmol/L, (26.9±5.7) μmol/L] (p<0.05, Fig. S3). No significant difference was observed for silicate among the three regions. Nutrient concentrations (nitrate, phosphate, and silicate) generally showed similar spatial distributions as salinity (p<0.01), with higher values in the upper layers of Region II and lower layers of Region III (Fig. S3). As for the vertical profiles of nutrient concentrations, increasing trends with greater water depth were observed (p<0.01, Fig. S3). The N/P, Si/P, and N/Si ratios were around 8.7–21.8 (average 13.6±1.2), 32.0–90.6 (average 41.5±5.7), and 0.1–0.5 (average 0.3±0.0), respectively. There was no significant difference in N/P ratios among the three regions, but significantly higher Si/P and lower N/Si ratios in Region III and moderate Si/P and N/Si ratios in Region I (Figs S3 and S4). Differences in the vertical profiles of nutrient concentrations, the N/P, Si/P, and N/Si ratios showed no remarkable vertical variation (Fig. S4). According to the stoichiometric criteria for phytoplankton physiology (silicate concentration>2 μmol/L, nitrate concentration >1 μmol/L, phosphate concentration >0.1 μmol/L, 10<N/P ratio<22, Si/P ratio>10) (Justić et al., 1995), the nutrient concentrations of the study area [silicate, (85.6±7.4) μmol/L; nitrate, (28.5±4.1) μmol/L; phosphate, (2.1±0.3) μmol/L] were much higher than the algal nutrient minimum demand, and no potential nutrient limitation was observed in the study area [N/P ratio, 13.6±1.2; Si/P ratio, 41.7±3.3] (Fig. S4), indicating a non-nutrient-limited environment.

3.3 *Concentrations and distribution of phytoplankton pigments*

The concentration of Chl *a* is usually used to estimate phytoplankton crops. As shown in Fig. 4, Chl *a* concentrations ranged from 0 to 0.73 mg/m^3 with an average of (0.14±0.13) mg/m^3. Concentrations of Chl *a* in Region I [(0.17±0.18) mg/m^3] were much higher than the other two regions [Region II, (0.12±0.07) mg/m^3; Region III, (0.13±0.13) mg/m^3], which were similar with literature data (Table 3). Moreover, similar to the nutrient and hydrological data, different horizontal distribution trends existed between upper and lower layers (Fig. 4). In the upper layers, regions with high Chl *a* values were mainly distributed in the Sections D1 and D2 of Region I and Section D5 of Region III. In contrast, Section D3 of Region 2 demonstrated high Chl *a* concentrations in the lower layers of the study area (Fig. 4). Moreover, surface phytoplankton crops of early summer (early January, this study) were comparable with reported data detected in the same sampling period but generally lower than those of middle and late summer (February to March, Table 3).

Vertically, the concentrations of Chl *a* decreased significantly with greater water depth (p<0.01), and subsurface maximum layers occurred in 25 stations. Phide-*a* and Phytin-*a* are primary degradation products of Chl *a*, which can be associated with the food web structure and the main predator. Variations of Phytin-*a* concentrations can be used to indicate the relative distribution of large zooplankton (e.g., krill and copepods), and Phide-*a* is an indicator of the distribution of smaller zooplankton (e.g., protozoa) (Jeffrey et al., 1997). In this study, ranges of Phide-*a* concentration varied from 0 to 0.34 mg/m^3 [average (0.05±0.12) mg/m^3], with the lowest values in Region II and highest values in Region III (Fig. S5). The Phytin-*a* concentration ranged from 0 to 0.03 mg/m^3 [(0.01±0.02) mg/m^3] (Fig. S5). Similar to the vertical profiles of Chl *a* concentration, the Phide-*a* and Phytin-*a* both showed decreasing trends with increasing water column depths. The Fuco [(0.68±1.01) mg/m^3], Chl c_2 [(0.35±0.50) mg/m^3] and Chl c_3 [(0.18±0.23) mg/m^3] were the most abundant diagnostic pigments in this study. Their spatial distribution patterns in different layers was similar to Chl *a* (Fig. S5). In comparison, the concentrations of Peri [(0±0.01) mg/m^3], Allo [(0.01±0.03) mg/m^3], Zea [(<0.04) mg/m^3] and Chl *b* [(0.01±0.02) mg/m^3] were fairly low.

Spatial distributions of the integrated pigment concentrations in the water column are shown in Fig. 5. Higher concentrations of Chl *a* were found in the adjacent sea area of Antarctic Peninsula and South Orkney Island. The integrated Chl *a* concentration ranged from 8.9 mg/m^2 to 64.2 mg/m^2, with an average of 23.2 mg/m^2. The concentration of Phide-*a* [(7.0±11.1) mg/m^2] was higher than Phytin-*a* [(1.3±1.1) mg/m^2]. Both Phide-*a* and Phytin-*a* decreased significantly with higher offshore distance. Chl c_2 [(50.7±50.1) mg/m^2] and Fuco [(102.7±111.6) mg/m^2] were the most abundant chlorophyll and carotenoid in the study area (Figs 5d and e), and lower average values were observed in Chl c_3 [(28.6±23.4) mg/m^2] and Chl *b* [(2.0±1.2) mg/m^2]. Generally, most of the abundant diagnostic pigments showed similar spatial distributions (e.g., Chl c_2, Chl c_3, and Fuco, r>0.84, p<0.01), with higher values in areas adjacent to the islands and lower values in Region II (Figs 5d–f). In contrast, the diagnostic pigments (e.g., Chl *b* [(2.0±1.2) mg/m^2], Allo [(1.8±7.5) mg/m^2], Peri [(0.4±1.6) mg/m^2], and Zea [(0.2±0.5) mg/m^2] had very low concentrations and showed no obvious spatial distribution patterns.

3.4 *Phytoplankton taxonomic composition based on CHEMTAX*

The calculated phytoplankton taxonomic groups based on the CHEMTAX model is shown in Figs 4 and 5. Generally, diatoms (63%±21%) and *P. antarctica* (31%±18%) were the two dominant algae in the study area. The ranges and average values of calculated six phytoplankton taxonomic groups in different layers are shown in Table S3. Similar to the Chl *a* concentration, relative proportions of diatoms showed decreasing trend offshore, with higher values in Regions I (72%±5%) and III (76%±6%) and lower value in Region II (59%±4%) (p<0.05) (Fig. 3a). In the lower layers, the relative abundance of diatoms was higher in stations near Elephant Island and the Philippine Ridge (Fig. 4). The percentage of diatoms generally showed a decreasing trend with greater water depth (p<0.01, Fig. 4). As for *P. antarctica*, higher average values were found in Regions I (25%±5%) and II (35%±12%) and the lowest average value in Region III (19%±6%)

(Fig. 3b). In contrast to the diatoms, *P. antarctica* showed an increasing trend with water column depth (p<0.01) (Fig. 4). Furthermore, in most stations, the dominant species changed from diatoms to *P. antarctica* in the layers deeper than 75 m (Fig. 4). Compared with the dominant diatoms and *P. antarctica*, green flagellates (4%±5%), cryptophyta (1%±3%), dinoflagellates (1%±4%) and cyanobacteria (1%±5%) occupied only a minor proportion. Spatially, the green flagellates were mainly distributed in the upper layers of the South Scotia Ridge, cryptophyta occurred only in the upper layer of the Region III, and dinoflagellates (1%±4%) and cyanobacteria (1%±5%) were found only sporadically in lower layers of certain sites (Fig. 4). As for the vertical profiles, the relative proportion of green flagellates decreased with increasing water depth, while the cryptophyta, dinoflagellates, and cyanobacteria showed an increasing trend (p<0.05) (Table S3).

3.5 *Phytoplankton response to environmental drivers*

An RDA was conducted to reveal the potential response of phytoplankton crops and taxonomic groups to environmental factors of surface water (Fig. 6). Water environment factors, including MLD, stability of water column, MWC, PAR, salinity, and nutrient concentrations and structure, illustrated various contributions to the phytoplankton crops and taxonomic composition–environment relationships. The water environmental factors covered by the first two RDA axes explained 79.6% and 5.6% of the total variance in the phytoplankton crops and taxonomic composition (Fig. 6). These results indicate that the physical environment (e.g., PAR, MLD, salinity, $E_{stability}$) and nutrient compositions have a significant relationship with the phytoplankton species composition, and these terms together provided 85.2% of the total RDA explanatory power (Fig. 6). As the RDAs showed, the PAR, Si/P and Si/N ratios, $E_{stability}$, and MWC had a positive influence on the percentage of diatoms and Chl *a* and its degradation product concentration. In comparison, the water temperature, salinity, MLD, nutrient concentrations, and N/P and N/Si ratios showed a positive influence on the *P. antarctica* and green flagellate proportions (Fig. 6).

As for the whole water column, the Pearson linear correlations analysis was used to detect the relationship between the studied parameters (Table S4). The results suggested that the water temperature, MWC, $E_{stability}$, Si/P ratio, and percentages of diatoms were significantly correlated with concentrations of Chl *a* and its degradation products (p<0.01, Table S4). In contrast, the salinity, proportions of dinoflagellates and *P. antarctica*, concen-

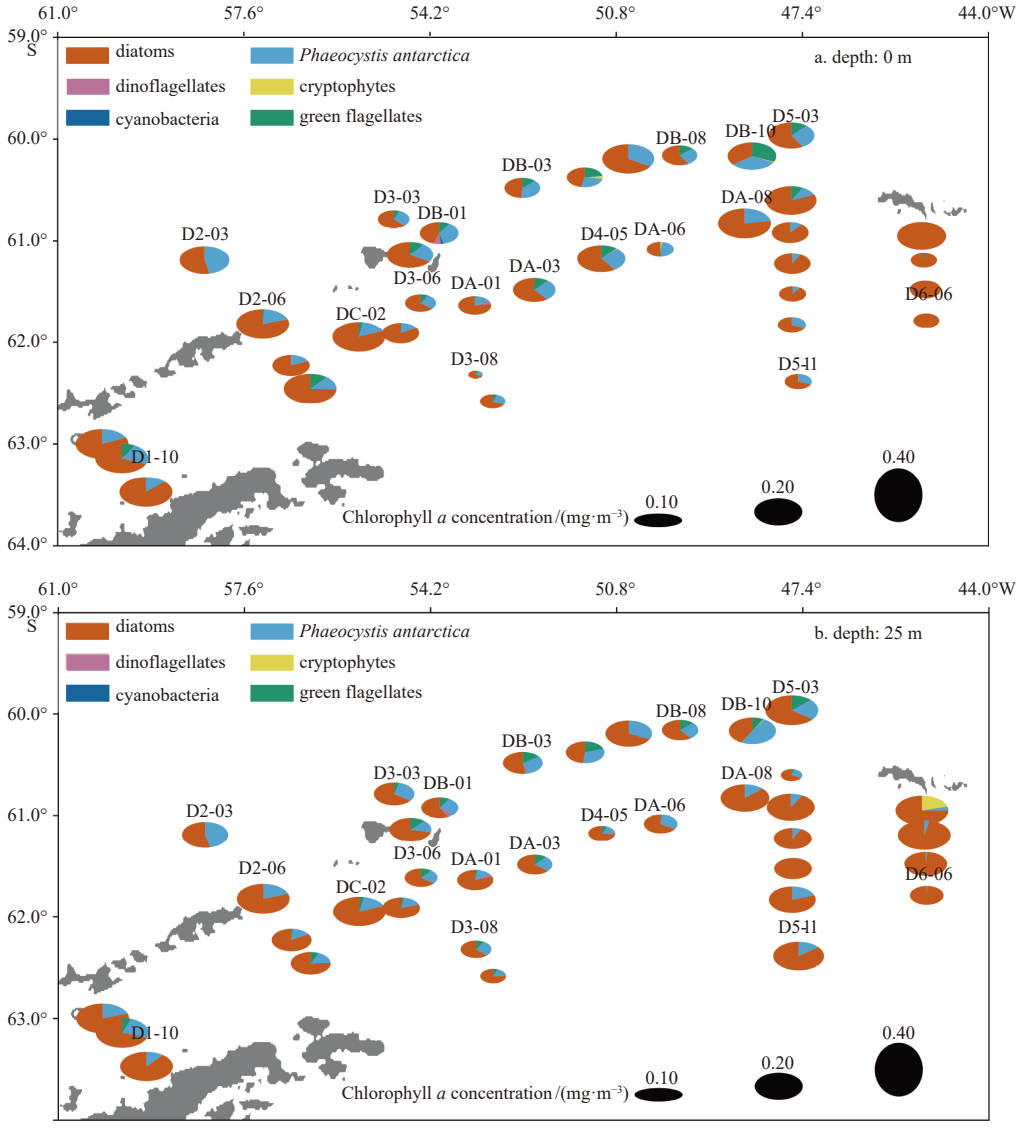

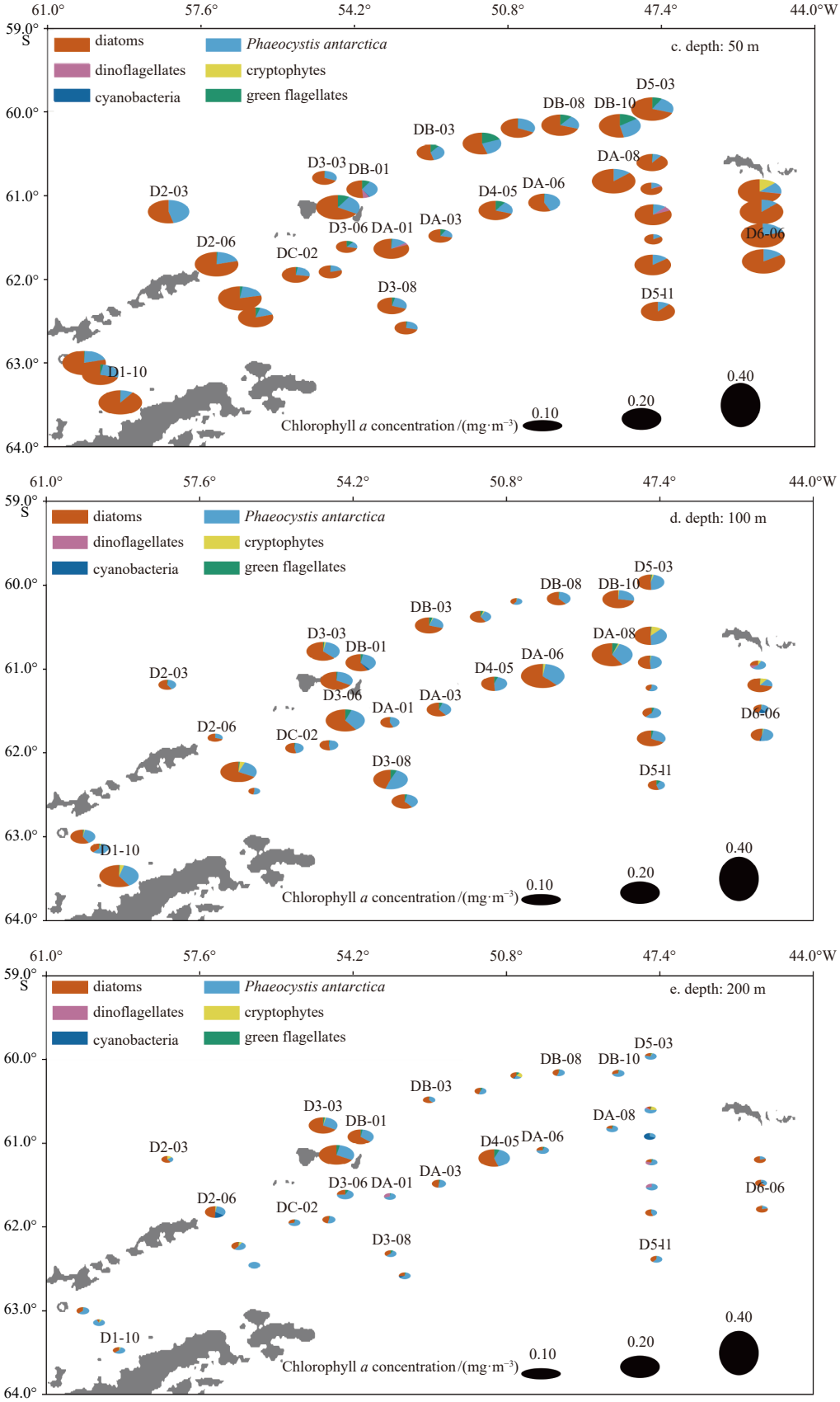

Fig. 4. Distributions of phytoplankton crops and taxonomic composition in the water column (0 m (a), 25 m (b), 50 m (c), 100 m (d), and 200 m (e)) in the northeastern Antarctic Peninsula. The pie graph diameter is proportional to the mean concentration of total chlorophyll *a*, and the composition reflects the contributions of different phytoplankton groups to chlorophyll *a* determined from CHEMTAX calculations.

Table 3. Comparisons of the average (± standard deviation) and ranges (in parenthesis) of surface Chl *a* concentrations, average proportions of phytoplankton taxonomic groups calculated by CHEMTAX, and nutrient concentrations in this study and former studies

Data sources	Sampling period	Study area	Nitrate/ ($\mu mol \cdot L^{-1}$)	Phosphate/ ($\mu mol \cdot L^{-1}$)	Silicate/ ($\mu mol \cdot L^{-1}$)	Surface Chl *a*/ ($mg \cdot m^{-3}$)	Average proportions of major phytoplankton taxonomic groups
This study	4–13 Jan. 2016 (early summer)	Region I	28.3±3.3	2.1±0.2	85.7±5.2	0.26±0.19 (0.06–0.72)	diatoms: ~64%, *P. antarctica* : ~32%, green flagellates: ~2%, others:~2%;
Russo et al. (2018)	12 Feb.–3 Mar. 2013 (late summer)	Bransfield and Gerlache Straits (Region I)	25.8	1.8	36.0	(0.4–1.6)	diatoms:~55%, *P. antarctica*: ~15%, chemotaxonomic group*:~15%, cryptophytes:~15%;
García-Muñoz et al. (2013)	8–27 Jan. 2010 (early and middle summer)	South Shetland Islands adjacent sea area (Region I)	29.6±3.1	1.8±0.1	70.1±7.9	0.4	diatoms:~80%, *P. antarctica*: ~10%, dinoflagellates and prasinophytes: ~10%;
Mendes et al. (2012)	Feb.– Mar. 2008 (late summer)	Bransfield Strait and adjacent sea area (Region I)	–	–	–	(0.5–1.2)	diatoms:~60%, chemotaxonomic Group*:~30%, greenflagellates, *P. antarctica* and others: ~10%;
Rodriguez et al. (2002)	Jan. 1996 (mainly early and middle summer)	Gerlache and Bransfield Straits (Region I)	–	–	–	(0.5–7)	diatoms and flagellates dominated;
This study	31 Dec. 2015–14 Jan. 2016 (early summer)	Region II	29.8±2.5	2.2±0.1	85.6±7.0	0.13±0.06 (0.01–0.24)	diatoms: ~57%, *P. antarctica*: ~35%, green flagellates: ~6%, others:~2%;
Mendes et al. (2018)	25 Feb.–1 Mar. 2013 (late summer)	Region II	27.5±1.2	1.4±0.1	29.3±3.8	(0.98–1.37)	dinoflagellates:~41%, diatoms: ~28%, *P. antarctica*: ~16%, cryptophytes:~12%, green flagellates: ~4%;
This study	29 Dec. 2015–11 Jan. 2016 (early summer)	Region III	26.9±5.7	2.0±0.4	85.5±9.5	0.13±0.10 (0.06–0.38)	diatoms: ~70%, *P. antarctica* : ~24%, cryptophytes:~4%, green flagellates: ~1%;
Nunes et al. (2019)	2 Jan.–12 Feb. 2015 (mainly middle and late summer)	south of the South Orkney Islands (Region III)	27.5±3.2	2.1±0.2	47.3±4.6	(0.1–0.4)	*P. antarctica*: ~50%, diatoms: ~25%, dinoflagellates:~15%, cryptophytes:~5%, pelagophytes: ~5%

Note: *, Peridinin-lacking autotrophic dinoflagellates and diatoms with Chl c_3.

trations of phosphate, nitrate, and silicate, and N/P ratio were significantly negatively correlated to the phytoplankton crops (p<0.01, Table S4). With respect to the phytoplankton taxonomic composition, the dominant diatoms positively correlated with MWC (r=0.20, p<0.01), $E_{stability}$ (r=0.20, p<0.01), and Si/P ratio (r=0.34, p<0.01), and negatively correlated with MLD (r=0.17, p<0.05), salinity (r=0.57, p<0.01), nutrient concentrations (r>0.39, p<0.01), and N/Si ratio (r=0.37, p<0.01). By contrast, the second most abundant algae (*P. antarctica*) was positively correlated with MLD (r=0.17, p<0.01), salinity (r=0.52, p<0.01), nutrient concentration (r>0.57, p<0.01), and N/Si ratio (r=0.37, p<0.01), and negatively correlated with water temperature (r=0.18, p<0.01), $E_{stability}$, MWC, and Si/P ratio (r=0.34, p<0.01).

4 Discussion

4.1 *Regionally oceanographic and hydrological characteristics*

The Southern Ocean is characterized by high hydrographic variability, and the ecosystem changes therein are linked to the regional intrinsic physicochemical properties and current circulation patterns. As shown by the cluster analyses, distinct environmental (oceanographic and hydrological) characteristics of three regions are accompanied by the variant phytoplankton crops and taxonomic composition therein (Figs 3 and 7).

Region I is the nearest area to the Antarctic Peninsula and the oceanographic environment is regulated by the warm and fresh water derived from the Antarctic Circumpolar Current (ACC, Fig. S2), Transitional Bellingshausen Water (TBW) (Fig. 2a), and the cold and saline coastal current (CC, regulated by glacial melt water, Fig. S6), which broadly exists over the continental shelf (Barlett et al., 2018; Thompson et al., 2009) (Fig. 1). The high salinity indicated that Region I was less affected by sea ice melt water (MWC, 0.7%±0.4%) (with the exception of Station D2-03, which was regulated by the ACC, Fig. 2c). Additionally, the fairly constant water density of the shallow water suggested moderate water mixing leading to a moderate MLD [(63±20) m] and slight weak water stability, especially in the basin region (Figs 1 and 2b). The relatively warm water of the Antarctic Slope Front (ASF) (Fig. S7) combined with the ACC dominated the shallow waters of Region II, where its hydrological conditions were modified due to the interaction with strong ACC in the region over and surrounding the South Scotia Ridge (Thompson et al., 2009). The high salinity of Region II indicated that the effect of MW was also limited (MWC, 0.9%±0.7%) (Figs 2c, Fig. S2b), and the water density showed a smoothly increasing trend with greater water depth, indicating strong water mixing and low stability (Figs 2 and 7). Region III had the lowest water temperature and salinity in the study area (p < 0.01). Lower temperature and salinity shal-

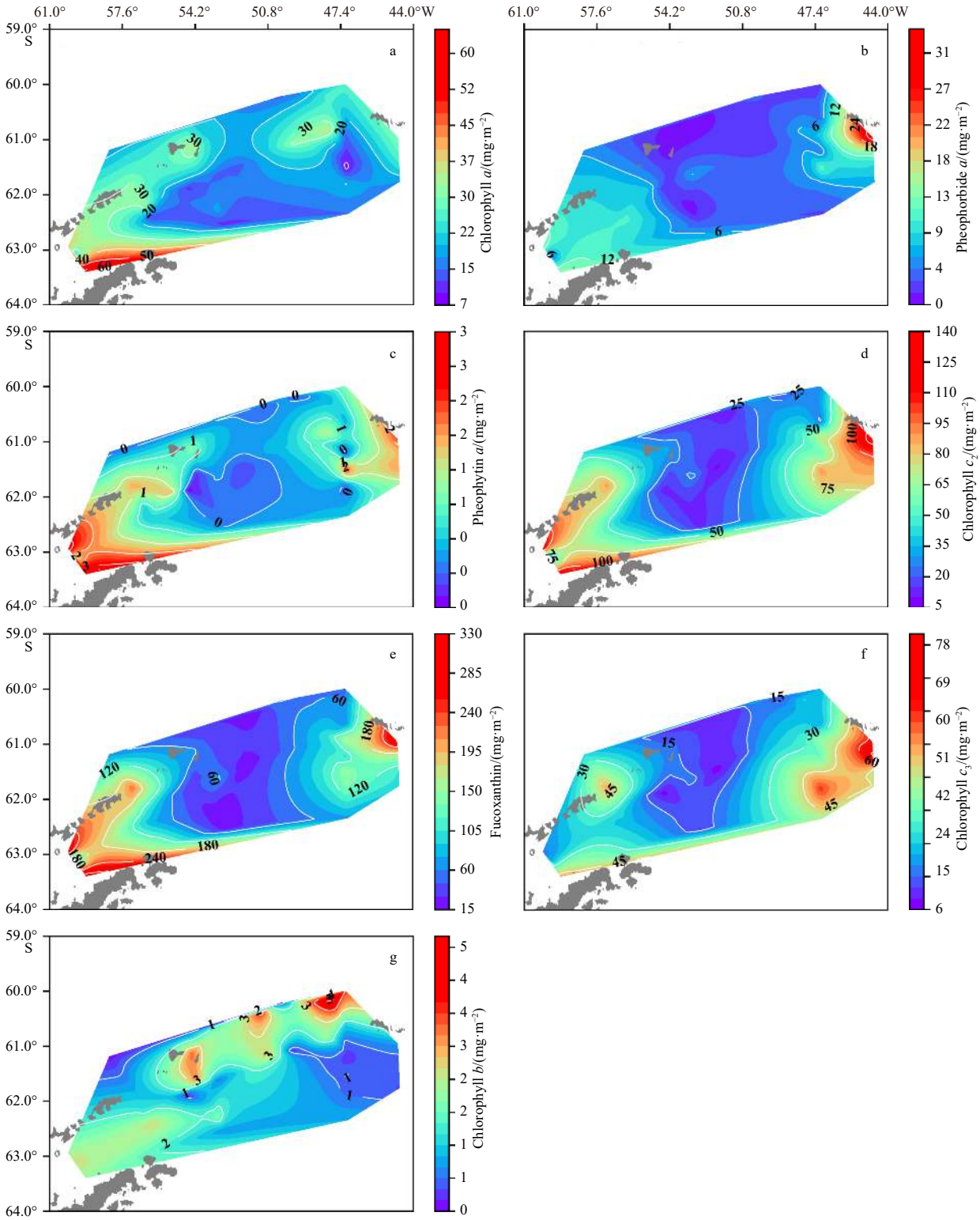

Fig. 5. Spatial distributions of the integrated concentration of chlorophyll *a* (a) and its degradation products (b and c), and diagnostic pigments (d–g).

low waters surrounding the South Orkney Island (Figs 2a, Fig. S7), suggested stronger influence of locally formed winter water and sea ice melt water (MWC, >2%) compared with the other two regions (Fig. 2c). Additionally, the cold-water Weddell Front (WF) dominated the deep layers in the more open sea area (Fig. S2b). Due to the widely developed and higher contribution of sea ice melt water, a steeper slope of water physical properties with greater water depth resulted in much stronger water column stability and shallower MLD in Region III (Figs 2b and d). In contrast, stronger water mass mixing and low water stability led to a gradual thermocline and much deeper MLD in the other two regions (Figs 2a and 3e).

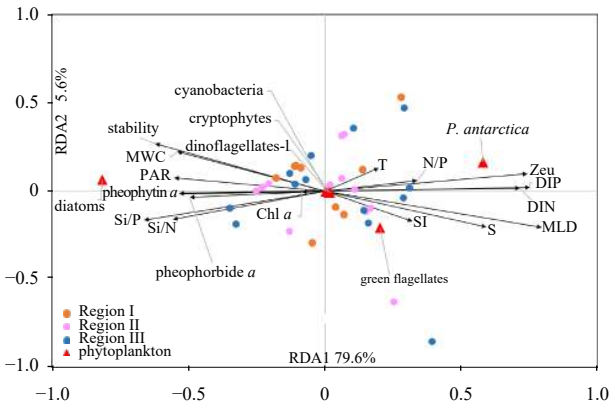

Fig. 6. Redundancy analysis (RDA) ordination plot for the first two principal dimensions of the relationships between the phytoplankton crops and taxonomic composition with environmental parameters in surface water. The environmental factors included in the first two RDA axes explain 85.2% of the total variance in the phytoplankton crops and taxonomic composition. Arrows indicate environmental variables. Red triangles refer to absolute contributions of phytoplankton groups. Orange, pink, and blue dots indicate Regions I, II, and II, respectively.

Current circulation near the tip of the Antarctic Peninsula not only conducts the thermohaline structures, but also influences the dissolved nutrient status and further ecosystem dynamics. The ASF, CC, and WF are considered to melt the underside of ice shelves and could transport substantial Antarctic krill and nutrients (Dotto et al., 2016; Fahrbach et al., 1994), especially for WF, which is considered to be Fe enriched (Ardelan et al., 2010). Correspondingly, higher nutrient concentrations (e.g. nitrate, phosphate, and silicate) were observed in Region II (50°–55°W, Fig. S3). In contrast, the ACC flows eastward through the Drake Passage to our study area and is believed to be Fe deficient (dissolved Fe, <0.5 nmol/L) (Hopkinson et al., 2007; Hewes et al., 2008). Additionally, the complex circulatory system of surface waters in Regions I and II produces many mesoscale processes, such as anticyclonic eddies, which have their own thermohaline structures and deep MLD, and become separated from adjacent currents (García-Muñoz et al., 2013; Heywood and Priddle, 1987; Sangrà et al., 2011, 2014; Thompson et al., 2009) (Fig. 2). For instance, a large-standing anticyclonic eddy (approximately 40 km in diameter, centered at 62°S and 54°W) maintained by regional topography and energy from strong shears of the ASF exists in region II (Thompson et al., 2009). This permanent feature of the surface circulation is dynamically significant for the mixing of water masses and dispersal of materials therein. For example, drifters deployed in the continental shelf east of the Antarctic Peninsula underwent remarkable oscillations (several months) which indicated significant eddy trapping (Thompson et al., 2009). The eddy could also trap phytoplankton for long periods of time and prolong their residence time in this region (Thompson et al., 2009), and even insulate the phytoplankton community from heavy grazing by zooplankton (e.g., krill) (Heywood and Priddle, 1987).

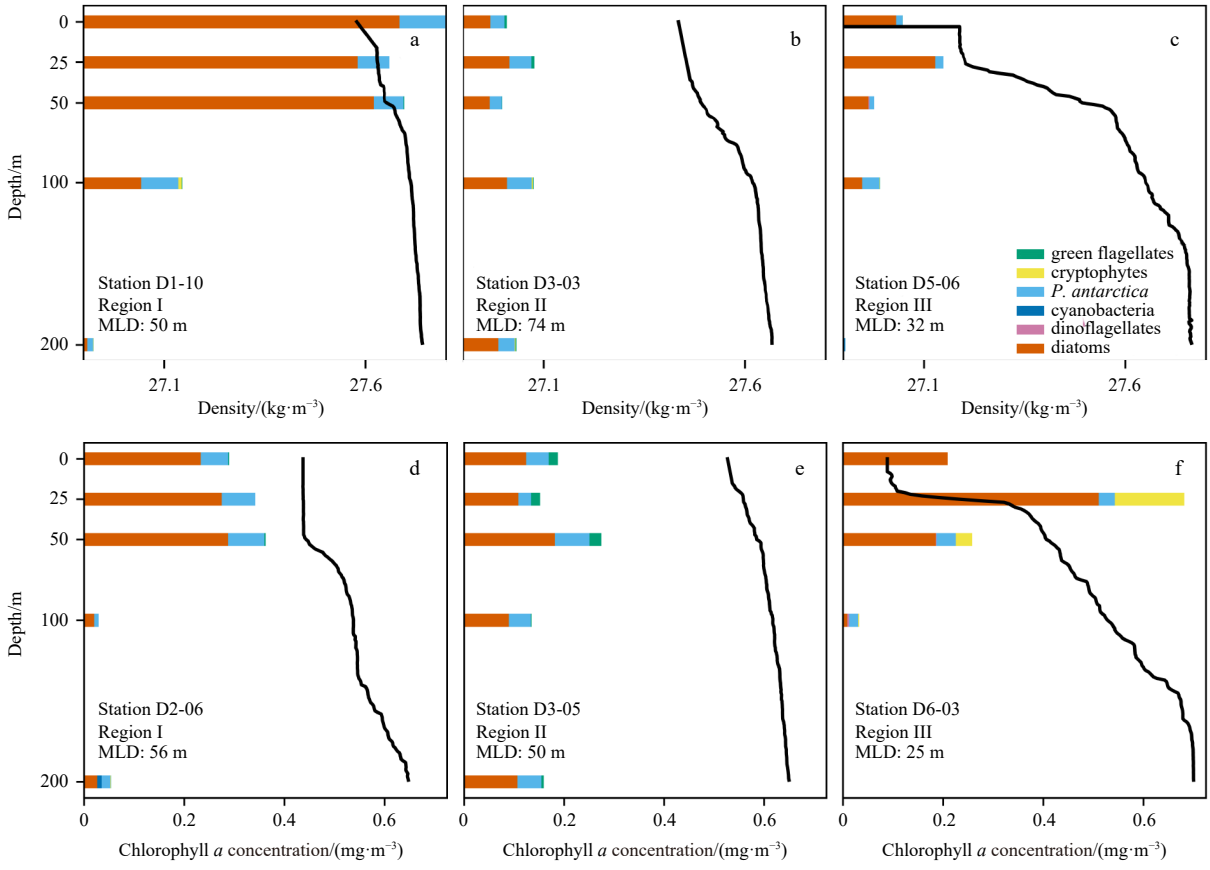

Fig. 7. Representative profiles of phytoplankton crops and taxonomic groups calculated by CHEMTAX at Region I (Stations D1-10 and D2-06), Region II (Stations D3-03 and D3-05), and Region III (Stations D5-06 and D6-03). The black lines indicate the density profiles of the respective stations.

4.2 *Interaction between nutrient status and phytoplankton*

Significant correlations between nutrient conditions and phytoplankton crops, taxonomic composition, and further herbivore activities indicate strong interactions among them (Fig. 6, Table S4). In the study area, the nutrient concentrations were significantly negatively correlated with total Chl *a* concentrations and herbivore feeding products (Fig. 6, Table S4). Similarly, comparing with previous studies (Table 3), lower phytoplankton crops is usually accompanied by higher nutrient stock (especially for silicate, Mendes et al., 2013). This phenomena could be attributed to the consumption of large amounts of dissolved nutrient stocks by phytoplankton growth (Westwood et al., 2010). In addition, due to the efficient supply of micronutrients (i.e., iron) and the much more stable water column in the coastal area of Regions I (South Shetland Island and Antarctic Peninsula) and III (South Orkney Island), higher phytoplankton crops [(25.6±15.8) mg/m^2, (23.2±13.8) mg/m^2] and subsequent strong feeding activities [Phytin-*a*, (1.6±1.1) mg/m^2, (1.8±1.3) mg/m^2] accompanied by the lowest nutrient stocks [phosphate, (2.1±0.2) μmol/L, (2.0±0.4) μmol/L; nitrate, (28.3±3.3) μmol/L, (26.9±5.7) μmol/L] were found in Regions I and III compared with Region II [Chl *a*, (21.6±5.7) mg/m^2; phosphate, (2.0±0.4) μmol/L; nitrate, (26.9±5.7) μmol/L]. Similarly, pretty high Chl *a* concentration (around 0.5–7 mg/m^3) was also reported near James Ross Island and in the Bransfield Strait (Mendes et al., 2012). Moreover, although the nutrient concentrations of deep water (>100 m) are comparable among the three regions (Figs S3a and b), shallower MLD in Regions I and III compared with Region II (p<0.01) would also limit the upwelling of nutrient-rich deep water, and further result in the lower nutrient concentration therein (Figs S3a and b). Furthermore, phytoplankton with different sizes and nutrient uptake efficiencies also have diverse preferences and tolerance to nutrient status (Gibb et al., 2001; Gibberd et al., 2013). For instance, diatoms favor silicate-enriched environments as silicate is an essential element for the formation of siliceous diatom shells, and is consistent with positive correlations between diatoms and Si/N ratios found in this study (Fig. 6). In contrast, *P. antarctica* and green flagellates could be much more adapted to nitrate- and phosphate-enriched environments with higher N/P (Arrigo et al., 1999) (Fig. 6). Despite the higher nutrient inventory of Region II (especially for nitrate and phosphate), the lowest Si/N and Si/P ratios in Region II (p<0.05) may partly contribute to the lower diatom percentage compared with that observed in the other two regions (Fig. 3).

Although the Fe concentration was not analyzed in this study, the MWC has been shown to be a good indicator for Fe-rich freshwater inputs in the continental marginal sea of the Antarctica continent (Costa et al., 2020; Mendes et al., 2018b; Wang et al., 2020; Zhang et al., 2019). In this study, although no significant correlation was observed between the MWC and Chl *a* concentrations due to complex hydrology conditions, negative relationships existed between MWC and *P. antarctica* percentage (r=–0.20, p<0.01). One possible reason is that nanophytoplankton (e.g., *P. antarctica* (<20 μm), cyanobacteria (1–2 μm), green flagellates (0.1–5 μm) and cryptophyta (6–20 μm)) with a small size and high specific surface area could favor their nutrient uptake, and thus have a competitive advantage under Fe-deficient environments (Gibb et al., 2001; Hassler et al., 2014). Also, the proportion of utilized Fe by the larger phytoplankton (e.g., diatoms (>20 μm)) increases in strongly stratified waters with higher MWC (Wang et al., 2020). Similarly, Mendes et al. (2012) reported ice melting processes would trigger growth of large diatoms in coastal sea area of James Ross Island. Based on the efficient Fe supplement from upwelling and glacial melt water, the Fe concentration of Region III was around three times higher than that of Region II (Ardelan et al., 2010; McGillicuddy et al., 2015; Sanchez et al., 2019). This may have thus resulted in the low diatom and high *P. antarctica* proportions in Region II, and vice versa in Region III (Fig. 3), which was consistent with another study carried out in the South Scotia and Philip Ridge during late summer (Mendes et al., 2018b). The high-Fe cyclonic ASF flows clockwise along the Powell Basin and to the south (Wang et al., 2020) (Fig. 1), likely contributed to the limited Fe supply to Region II (0.31–0.73 nmol/L) (McGillicuddy et al., 2015; Sanchez et al., 2019). As shown in Fig. 7a, a region with high Chl *a* concentrations centered at 49°W and 61°S in Region II, far from an island, result the horizontal mixing of an Fe-rich ASF with the well-stratified but Fe-poor ACC. Similar phenomena were also described within the western Weddell-Scotia Confluence region (Heywood et al, 2004; Von Gyldenfeldt et al., 2002). Thus, the northbound horizontal delivery of nutrients by the ASF and release of demanded Fe onto the shelf and ridge area of Region II may be an important point source driving high biomass in the pathway of the ASF.

4.3 *Effect of light intensity and water mixing on phytoplankton growth*

4.3.1 *Influence of light intensity*

Light intensity affected by the weather conditions has been considered to be the primary factor determining the phytoplankton crops and taxonomic composition (Arrigo et al., 1999; Hoppe et al., 2017; Mendes et al., 2012; Wojtasiewicz et al., 2019). In this study, based on the PAR and Zeu data calculated from remote sensing data, the influence of light intensity on the phytoplankton growth was also estimated. The regional variation in PAR was the same as that of Chl *a* concentrations, with Region I having the highest PAR and Chl *a* concentration while Region II had the lowest PAR and Chl *a* concentration (Fig. 3). Only in Region II, which was mainly an open sea area, did a significantly positive relationship exist between PAR and phytoplankton crops (r=0.52, p<0.05), indicating the important regulating effect of light radiation intensity on phytoplankton crops in the well-mixed water column with deep MLD. Moreover, combing with the historical literature (Table 3) and remote sensing data (https://hermes.acri.fr/index.php) in this study area (e.g., Regions I and II), we find a time lag (around one month) between the most lightful (December and January) and the most productive months (January and February). Although with the highest PAR during early summer (https://hermes.acri.fr/index.php) in the study area, the Chl *a* concentrations during early austral summer (i.e., December and January) was even slightly lower than those studies carried out during mid and late austral summer (i.e., February and March) (Table 3). Similar monthly discrepancies on primary production rates (i.e., Region I) were reported: higher carbon assimilation rates were found during February and March (0.93–3.38 mg/(mg·h), assimilated carbon mass by per milligram Chl *a* per hour) and lower values during January (0.30–2.02 mg/(mg·h), assimilated carbon mass by per milligram Chl *a* per hour) (Russo et al., 2018 and references therein). This phenomenon probably was a compromise between light condition and water column structure, especially in this strong hydrodynamic environment.

Positive correlations were observed across the entire study area between PAR and diatoms in the water column (r=0.52, p<0.01), while a negative relationship with *P. antarctica* (r=–0.58, p<0.01) and green flagellates (r=–0.41, p<0.05) was observed (Fig. 6). This phenomenon is consistent with previous studies in the Ross

Sea (Rozema et al., 2017) and West Antarctic Peninsula adjacent sea area (Joy-Warren et al., 2019), and could be attributed to the differences in photophysiology of diatoms and *P. antarctica*. For example, compared with *P. antarctica*, diatoms could produce less photosynthetic pigment and higher photoprotective pigment per cell, and thus are far less susceptible to photoinhibition and could sustain competitive advantage under environment with high light levels (Arrigo et al., 1999; Villafañe et al., 2008). By contrast, the *P. antarctica* can produce more light-harvesting pigments per cell, and are susceptible to photoinhibition, but could dominate waters where light levels are low (Alderkamp et al., 2010). This photophysiological characteristic may have contributed to the significantly lower percentage of diatoms (59%±4%) and higher percentage of *P.* antarctica (34%±5%) in Region II than Regions I and III (diatoms, 72%±6% and 76%±6%; *P. Antarctica*, 25%±5% and 20%±7%) (Fig. 3), and the vertically decreasing percentage of diatoms and increasing *P. antarctica* with greater water depth in the water column (Fig. 7). This was also supported by the monthly shift of the phytoplankton community from diatoms dominated to nanoflagellates dominated because the decreasing of light intensity from early summer to late summer (Table 3). Furthermore, cryptophyta, typically small flagellates that can successfully grow in highly illuminated conditions with shallow mixed layer (e.g. prevalence in the Gerlache Strait, Mendes et al., 2018a), also appeared in the upper layers of certain stations of Region III (e.g., Station D6-03, 16%) with higher PAR and strong water column stratification (Figs 2 and 4).

4.3.2 *Influence of water mixing*

Water stratification and mixing, which play an important role in shaping habitat environments (e.g., $E_{stability}$, Zeu, and MLD), are also limiting factors for the vertical distribution of phytoplankton crops and taxonomic composition (Cai et al., 2003; Hoppe et al., 2017; Mendes et al., 2012; Wojtasiewicz et al., 2019; Zhang et al., 2014, 2019). In this study, $E_{stability}$ was significantly positively and negatively correlated with MWC (r=0.94, p<0.01) and MLD (r=–0.67, p<0.01), respectively, indicating the more MW contribution and shallower MLD, the higher the water stability. In other words, the melt water has a high concentration of dissolved iron, so the Fe limit may be lifted in high stability waters columns (Costa et al., 2020; Mendes et al., 2018a; Wang et al., 2020). Three regions both received considerable MW inputs; however, mesoscale processes such as anticyclonic eddies (e.g., approximately 40 km in diameter, centered at 62°S and 54°W) maintained by regional topography and energy from strong shears of the ASF exist in Region II (Thompson et al., 2009) resulting in stronger mixing and the most unstable water environment in this region (deepest MLD and lowest $E_{stability}$). In this study, although no significant statistical relationship was found between $E_{stability}$ (or MLD) and phytoplankton crops, a stable water environment favors the growth of phytoplankton (Mendes et al., 2012) which is consistent with our observations of lower Chl *a* concentration in Region II where the water stability was lowest (Figs 2f and 5a).

Moreover, $E_{stability}$ and MLD showed significant correlation with the percentage of diatoms (r=0.20, p<0.01; r=–0.53, p<0.01), and inverse correlation with *P. antarctica* (r=–0.20, p<0.01; r=0.48, p<0.01) and green flagellates (r=–0.44, p<0.01; r=0.41, p<0.01) (Fig. 8). The vertical profiles of phytoplankton crops and taxonomic composition demonstrated obvious differences among stable and unstable water columns (Fig. 7). In the well-mixed water with deep MLD, the phytoplankton could be physically carried up and down and even below the Zeu depth, and the induced possible light limitation and unstable environments may result in a constant (0–200 m) but low crops having high and constant nanophytoplankton proportion in the water column (e.g., Stations D3-03 and D3-05 of Region II, Fig. 7). This is in line with dominance of nanoflagellates (e.g. cryptophytes and *P. antarctica*) in the open-ocean area of Weddell Sea (Mendes et al., 2012). In contrast, a high and dynamically decreasing crops below the mixed layer was observed in the water column with strong stratification and high stability, where the dominant phytoplankton changed from diatoms to *P. antarctica* (e.g., Stations D1-10 and D2-06 of Region I, Stations D5-06 and D6-03 of Region III, Fig. 7). The vertical changes of algal crops and taxonomic composition should be attributed to the rapid light attenuation caused by strong water stratification, as suggested by the negative relationship between $E_{stability}$ and Zeu (r=–0.84, p<0.01). Additionally, the slope of linear regression between the sum of Phytin-*a* and Phide-*a* concentration with Chl *a* concentration is a strong indicator of grazing pressure (Mendes et al., 2012). Although no significant correlation was found in the high Chl *a* part (Chl *a* concentration>0.16 mg/m^3) of Region II, the concentration of degradation products was significantly higher than that of the low Chl *a* part (Chl *a* concentration<0.16 mg/m^3) (p < 0.01). The feeding activity of the stations with low Chl *a* concentrations (k=0.08) was much lower than that of the whole Region II (k=0.22) (Fig. 9b), which confirms that zooplankton has patchy distribution characteristics similar to phytoplankton (Jeffrey et al., 1997). The lower slope and concentrations of Chl *a* degradation products in the well-mixed (low Chl *a* concentration) water column indicates weak feeding activities by herbivorous zooplankton in Region II (Figs 3 and 9).

4.4 *Perspective in evolution of the phytoplankton taxonomic composition and its ecological effect*

As the northernmost region of Antarctica, the Antarctic Peninsula with limited glaciers is suffering rapid warming (more than twice as fast as the global average), accelerated retreat rates of sea ice, and attenuation of glaciers during the past decades, due to anthropogenic activity and natural circulation variability (Clem et al., 2020; Cook et al., 2016; Martinson et al., 2008; Rozema et al., 2017; Stammerjohn et al., 2008; Turner et al., 2017). Simultaneously, significantly earlier sea ice retreating

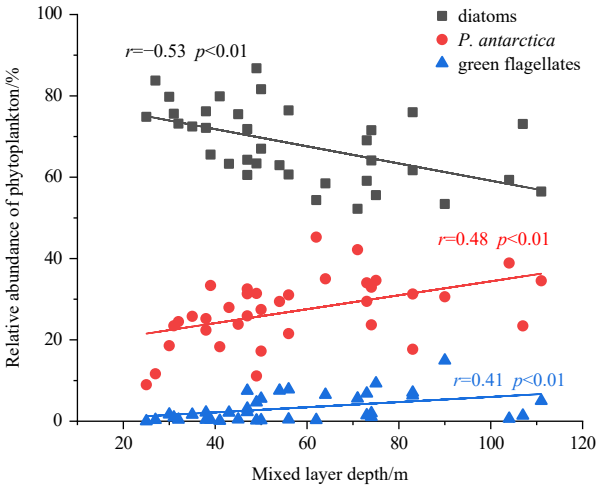

Fig. 8. Significant correlations between the mixed layer depth and the relative abundance of diatoms, *P. antarctica* and green flagellates.

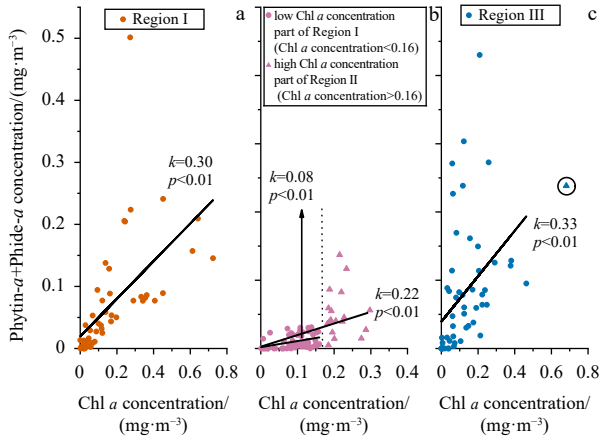

Fig. 9. Linear regressions of chlorophyll *a* (Chl *a*) concentrations and its degradation products (the sum of pheophorbide *a* (Phide-*a*) and pheophytin *a* (Phytin-*a*)) in three regions. The slope represents the grazing pressure with a steeper slope suggesting stronger feeding activities. Region III (c) has the highest slope (k=0.33, extreme value (blue triangle) is removed from calculation), the slope of Region I (a) is medium (k=0.30), and the slope of Region II (b) is the lowest (k=0.20). If only considering the stations with low Chl *a* concentration (<0.16 mg/m^3) of Region II, the slope (k=0.08) is much lower than that of the whole Region II.

(around 1 month), later sea ice advancing (around 2 months), and shortening of sea ice duration (around 3 months) in the Antarctic Peninsula regions were also reported through a 26 a period observation study (Stammerjohn et al., 2008). Austral summer is the most suitable season for phytoplankton growth and contributes nearly the whole year's primary productivity in the continental marginal sea of Antarctica (Park et al., 2010). To track the succession of the phytoplankton taxonomic groups under climate change, it is important to explore the trends and monthly and annual variations of the phytoplankton composition, especially during the austral summer.

As discussed in previous sections, the study area is a sensitive region of ice–sea interactions, which could induce various changes in a variety of environmental drivers such as MLD, light conditions, and micronutrient inputs. According to previous studies, the schematic of the annual evolution of past phytoplankton taxonomic groups is presented in Fig. 10a. However, in the future, the occurrence of phenomena mentioned above could significantly affect the marine ecosystem and biological carbon pump therein. In early spring with relatively low light intensity, the increasing temperature of air and surface seawater could lead to earlier retreating of sea ice and melt water input, and result in a shallow MLD with Fe-rich upper-layer water. However, due to the light limitation in early spring, the phytoplankton crops would still be low, which is also a premature consumption and waste of this Fe-rich water (Fig. 10b). In late spring and the early summer, the influence of the increasing light intensity and continuous glacial melt water input could cause diatom blooms to occur earlier. The diatoms could contribute around 57%–80% to the phytoplankton community during early summer (Table 3). However, due to the premature consumption and loss of Fe-rich sea ice melt water in spring, the Fe availability may become worse and water stratification may weaken in the coastal region, resulting in a much shorter period of diatom blooms in early

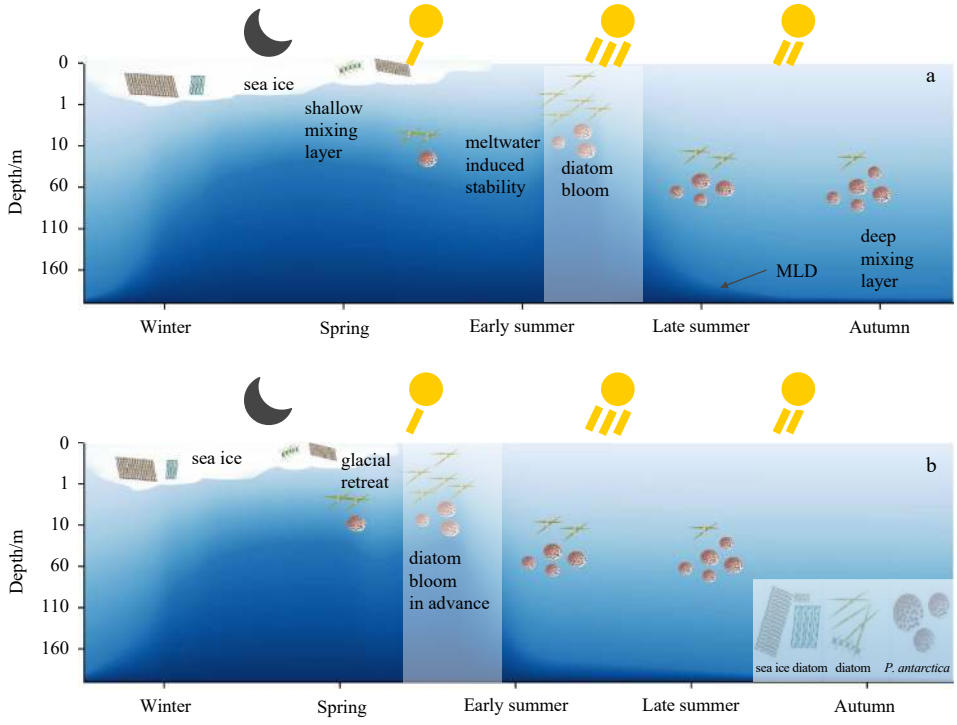

Fig. 10. Schematic model of past (García-Muñoz et al., 2013; Gonçalves-Araujo et al., 2015; Lovenduski and Gruber, 2005; Mendes et al., 2012; Nunes et al., 2019; Reiss et al., 2009; Russo et al., 2018) and future phytoplankton taxonomic composition under changing environments in the northeastern Antarctic Peninsula. The horizontal axis shows how marine environmental factors change temporally in the Antarctic Peninsula and its influence on phytoplankton taxonomic composition. The depth of the mixed layer is shown by the density change from light blue to dark blue.

summer (Fig. 10b). After that, with the continuously decreasing sea ice melt water input and strong wind mixing, a deeper MLD with weak water column stability could significantly favor the growth of smaller phytoplankton in the remaining lighting time during the year (Fig. 10b). This is supported by the quickly shift (from simple to complex) of phytoplankton taxonomic composition from early summer to late summer (Table 3). As shown in Table 3, the first two major taxonomic groups could account for more than 90% of the total phytoplankton community during early summer. In contrast, the groups only accounted for around 70% in late summer, but the proportion of smaller phytoplankton (dinoflagellates, cryptophyta and *P. antarctica*) increased significantly (e.g., Region I, 36%–45%; Region II, 43%–72%; Region III, 30%–75%).

With the shortening of sea ice duration, the period with favorable environmental conditions (Fe-rich and shallower MLD) for large diatom blooms is continuously shortening, and the period with a deep MLD and Fe-poor conditions, which is favorable for smaller cryptophyta and *P. antarctica*, is much longer (Fig. 10b). For example, the proportions of diatoms in Region I during early summer decreased from ~80% in January 2010 (García-Muñoz et al., 2013) to ~64% in January 2016 (this study), and from ~60% in February and March 2008 (Mendes et al., 2012) to ~55% in February and March 2013 (Russo et al., 2018) during late summer. Moreover, the proportions of smaller phytoplankton (e.g., *P. antarctica*, Chemotaxonomic group and others) in Region I during early summer increased from ~20% in January 2010 (García-Muñoz et al., 2013) to ~36% in January 2016 (this study), and from ~40% in February and March 2008 (Mendes et al., 2012) to ~45% in February and March 2013 (Russo et al., 2018) during late summer. Because part of the original large diatom-derived primary production would be replaced by a miniaturized phytoplankton taxonomic groups, the induced increasing biomass of small herbivores (e.g., copepods) and carbon-poor gelatinous zooplankton (e.g., salps) would lead to much lower biological pump efficiency (Costa et al., 2020; Wang et al., 2020) due to the lower carbon sequestration and deposition flux (Belcher et al., 2017; Moline et al., 2004; Murphy et al., 2007; Tréguer et al., 2018). Moreover, the decreasing crops and proportion of large diatoms, which are a favorable food and major source of energy for krill in spring and summer (suggested by a significantly correlated percentage of diatoms and products of feeding activities (e.g., Phytin-*a* and Phide-*a*) (r>0.46, p<0.01)), and an increasing abundance and relative proportion of nanophytoplankton (e.g., cryptophyta and *P. antarctica*), which are more efficiently grazed by carbon-poor salps (Cadée et al., 1992; Kerr et al., 2018b; Moline et al., 2004), may lead to the degeneration of the spawning ground for krill and even the migration of higher predators in the Antarctic Peninsula coastal region (Forcada et al., 2012). The changing of keystone species (diatoms and krill) would result in further changes in this marine ecosystem.

5 Conclusions

The northeastern Antarctic Peninsula is a region with complex environmental settings and variable phytoplankton taxonomic composition. In the coastal area (e.g., the South Orkney Island adjacent region and the region north of South Shetland Island), a strong intensity of PAR and high freshwater input from adjacent surface sea ice or glacial MW characterized the environmental settings therein. These environmental drivers promote water stability, induce shallow MLD, and relieve potential Fe limitations for phytoplankton growth. Consequently, significantly higher phytoplankton crops were observed in the coastal region of the Antarctic Peninsula and South Orkney Island. The relative proportion of diatoms, which favor high light intensity, a stable water column, and high-Fe waters, were more concentrated in this region. In offshore areas (e.g., Philip Ridge and South Scotia Ridge), despite much more abundant macronutrients, strong water mass interactions (ASF, WF, ACC, and eddies) provided an environment with a deep MLD and weak water column stability, and combined with relatively low PAR and limited Fe inputs. All of these environmental drivers contributed to low phytoplankton crops and less herbivore activities therein. Moreover, this environment favors the growth of small phytoplankton (e.g., *P. antarctica* and green flagellates), which have higher Fe-uptake efficiencies and are better adapted to light limitation and unstable environments compared to large diatoms. Since the Antarctic Peninsula has limited glaciers and is suffering rapid warming, it is experiencing an earlier sea ice retreat, shorter sea ice duration, and changes in the period and degree of water mixing (Stammerjohn et al., 2008). These changing ice–sea interactions would eventually lead to large changes to this ecosystem (e.g., miniaturization of the phytoplankton taxonomic groups) and a lower biological pump efficiency. More long-term observations are needed to further understand the ecosystem dynamics of this rapidly changing environment.

Acknowledgements

We thank the crews of the R/V *Xuelong* for their assistance with sample collection and the hydrological data provided by the Physical Ocean Group. We also thank the editor and two anonymous reviewers for their constructive comments.

References

Ackley S F, Buck K R, Taguchi S. 1979. Standing crop of algae in the sea ice of the Weddell Sea region. Deep-Sea Research Part A: Oceanographic Research Papers, 26(3): 269–281, doi: 10.1016/0198-0149(79)90024-4

Alderkamp A C, de Baar H J W, Visser R J W, et al. 2010. Can photoinhibition control phytoplankton abundance in deeply mixed water columns of the Southern Ocean?. Limnology and Oceanography, 55(3): 1248–1264, doi: 10.4319/lo.2010.55.3.1248 doi: 10.4319/lo.2010.55.3.1248

Ardelan M V, Holm-Hansen O, Hewes C D, et al. 2010. Natural iron enrichment around the Antarctic Peninsula in the Southern Ocean. Biogeosciences, 7(1): 11–25, doi: 10.5194/bg-7-11-2010

Arrigo K R, Robinson D H, Worthen D L, et al. 1999. Phytoplankton community structure and the drawdown of nutrients and CO_2 in the Southern Ocean. Science, 283(5400): 365–367, doi: 10.1126/science.283.5400.365

Barlett E M R, Tosonotto G V, Piola A R, et al. 2018. On the temporal variability of intermediate and deep waters in the Western Basin of the Bransfield Strait. Deep-Sea Research Part II: Topical Studies in Oceanography, 149: 31–46, doi: 10.1016/j.dsr2.2017.12.010

Barlow R, Kyewalyanga M, Sessions H, et al. 2008. Phytoplankton pigments, functional types, and absorption properties in the Delagoa and Natal Bights of the Agulhas ecosystem. Estuarine, Coastal and Shelf Science, 80(2): 201–211, doi: 10.1016/j.ecss.2008.07.022

Belcher A, Tarling G A, Manno C, et al. 2017. The potential role of Antarctic krill faecal pellets in efficient carbon export at the marginal ice zone of the South Orkney Islands in spring. Polar Biology, 40(10): 2001–2013, doi: 10.1007/s00300-017-2118-z

Cadée G C, González H, Schnack-Schiel S B. 1992. Krill diet affects faecal string settling. Polar Biology, 12(1): 75–80, doi: 10.1007/BF00239967

Cai Yuming, Ning Xiuren, Zhu Genghai, et al. 2003. Size fractionated biomass and productivity of phytoplankton and new produc-

tion in the Prydz Bay and the adjacent Indian sector of the Southern Ocean during the austral summer of 1998/1999. Haiyang Xuebao, 27(4): 135–147

Carvalho F, Kohut J, Oliver M J, et al. 2016. Mixing and phytoplankton dynamics in a submarine canyon in the West Antarctic Peninsula. Journal of Geophysical Research: Oceans, 121(7): 5069–5083, doi: 10.1002/2016jc011650

Cheah W, Soppa M A, Wiegmann S, et al. 2017. Importance of deep mixing and silicic acid in regulating phytoplankton biomass and community in the iron-limited Antarctic Polar Front region in summer. Deep-Sea Research Part II: Topical Studies in Oceanography, 138: 74–85, doi: 10.1016/j.dsr2.2016.05.019

Clarke A, Murphy E J, Meredith M P, et al. 2007. Climate change and the marine ecosystem of the western Antarctic Peninsula. Philosophical Transactions of the Royal Society B, 362(1477): 149–166, doi: 10.1098/rstb.2006.1958

Clem K R, Fogt R L, Turner J, et al. 2020. Record warming at the South Pole during the past three decades. Nature Climate Change, 10(8): 762–770, doi: 10.1038/s41558-020-0815-z

Cook A J, Holland P R, Meredith M P, et al. 2016. Ocean forcing of glacier retreat in the western Antarctic Peninsula. Science, 353(6296): 283–286, doi: 10.1126/science.aae0017

Costa R R, Mendes C R B, Tavano V M, et al. 2020. Dynamics of an intense diatom bloom in the northern Antarctic Peninsula, February 2016. Limnology and Oceanography, 65(9): 2056–2075, doi: 10.1002/lno.11437

Deppeler S L, Davidson A T. 2017. Southern ocean phytoplankton in a changing climate. Frontiers in Marine Science, 4: 40, doi: 10.3389/fmars.2017.00040

Dotto T S, Kerr R, Mata M M, et al. 2016. Multidecadal freshening and lightening in the deep waters of the Bransfield Strait, Antarctica. Journal of Geophysical Research: Oceans, 121(6): 3741–3756, doi: 10.1002/2015jc011228

Ducklow H W, Schofield O, Vernet M, et al. 2012. Multiscale control of bacterial production by phytoplankton dynamics and sea ice along the western Antarctic Peninsula: A regional and decadal investigation. Journal of Marine Systems, 98–99: 26–39, doi: 10.1016/j.jmarsys.2012.03.003

Fahrbach E, Rohardt G, Schröder M, et al. 1994. Transport and structure of the Weddell Gyre. Annales Geophysicae, 12(9): 840–855, doi: 10.1007/s00585-994-0840-7

Forcada J, Trathan P N, Boveng P L, et al. 2012. Responses of Antarctic pack-ice seals to environmental change and increasing krill fishing. Biological Conservation, 149(1): 40–50, doi: 10.1016/j.biocon.2012.02.002

García-Muñoz C, Lubián L M, García C M, et al. 2013. A mesoscale study of phytoplankton assemblages around the South Shetland Islands (Antarctica). Polar Biology, 36(8): 1107–1123, doi: 10.1007/s00300-013-1333-5

Garibotti I A, Vernet M, Kozlowski W A, et al. 2003. Composition and biomass of phytoplankton assemblages in coastal Antarctic waters: a comparison of chemotaxonomic and microscopic analyses. Marine Ecology Progress Series, 247: 27–42, doi: 10.3354/meps247027

Garibotti I A, Vernet M, Smith R C, et al. 2005. Interannual variability in the distribution of the phytoplankton standing stock across the seasonal sea-ice zone west of the Antarctic Peninsula. Journal of Plankton Research, 27(8): 825–843, doi: 10.1093/plankt/fbi056

Gibb S, Cummings D, Irigoien X, et al. 2001. Phytoplankton pigment chemotaxonomy of the northeastern Atlantic. Deep-Sea Research Part II: Topical Studies in Oceanography, 48(4–5): 795–823, doi: 10.1016/S0967-0645(00)00098-9

Gibberd M J, Kean E, Barlow R, et al. 2013. Phytoplankton chemotaxonomy in the Atlantic sector of the Southern Ocean during late summer 2009. Deep-Sea Research Part I: Oceanographic Research Papers, 78: 70–78, doi: 10.1016/j.dsr.2013.04.007

Gonçalves-Araujo R, de Souza M S, Tavano V M, et al. 2015. Influence of oceanographic features on spatial and interannual variability of phytoplankton in the Bransfield Strait, Antarctica. Journal of Marine Systems, 142: 1–15, doi: 10.1016/j.jmarsys.2014.09.007

Grasshoff K, Kremling K, Ehrhardt M. 1999. Methods of Seawater Analysis. 3rd ed. New York, NY, USA: Wiley-VCH, doi: 10.1002/9783527613984.ch27

Hassler C S, Ridgway K R, Bowie A R, et al. 2014. Primary productivity induced by iron and nitrogen in the Tasman Sea: an overview of the PINTS expedition. Marine and Freshwater Research, 65(6): 517–537, doi: 10.1071/MF13137

Hewes C D, Reiss C S, Kahru M, et al. 2008. Control of phytoplankton biomass by dilution and mixed layer depth in the western Weddell-Scotia Confluence. Marine Ecology Progress Series, 366: 15–29, doi: 10.3354/meps07515

Heywood K J, Garabato A C N, Stevens D P, et al. 2004. On the fate of the Antarctic slope front and the origin of the Weddell front. Journal of Geophysical Research: Oceans, 109(C6): C06021, doi: 10.1029/2003jc002053

Heywood R B, Priddle J. 1987. Retention of phytoplankton by an eddy. Continental Shelf Research, 7(8): 937–955, doi: 10.1016/0278-4343(87)90007-0

Hopkinson B M, Mitchell B G, Reynolds R A, et al. 2007. Iron limitation across chlorophyll gradients in the southern Drake Passage: phytoplankton responses to iron addition and photosynthetic indicators of iron stress. Limnology and Oceanography, 52(6): 2540–2554, doi: 10.4319/lo.2007.52.6.2540

Hoppe C J M, Klaas C, Ossebaar S, et al. 2017. Controls of primary production in two phytoplankton blooms in the Antarctic Circumpolar Current. Deep-Sea Research Part II: Topical Studies in Oceanography, 138: 63–73, doi: 10.1016/j.dsr2.2015.10.005

Jeffrey S W, Mantoura R F, Wright S W. 1997. Phytoplankton Pigments in Oceanography: Guidelines to Modern Methods. Paris, France: UNESCO, doi: 10.1016/s0031-9422(97)00810-8

Joy-Warren H L, Van Dijken G L, Alderkamp A C, et al. 2019. Light is the primary driver of early season phytoplankton production along the western Antarctic Peninsula. Journal of Geophysical Research: Oceans, 124(11): 7375–7399, doi: 10.1029/2019jc015295

Justić D, Rabalais N N, Turner R E. 1995. Stoichiometric nutrient balance and origin of coastal eutrophication. Marine Pollution Bulletin, 30(1): 41–46, doi: 10.1016/0025-326x(94)00105-i

Kerr R, Goyet C, da Cunha L C, et al. 2018a. Carbonate system properties in the Gerlache Strait, northern Antarctic Peninsula (February 2015): II. Anthropogenic CO_2 and seawater acidification. Deep-Sea Research Part II: Topical Studies in Oceanography, 149: 182–192, doi: 10.1016/j.dsr2.2017.07.007

Kerr R, Mata M M, Mendes C R B, et al. 2018b. Northern Antarctic Peninsula: a marine climate hotspot of rapid changes on ecosystems and ocean dynamics. Deep-Sea Research Part II: Topical Studies in Oceanography, 149: 4–9, doi: 10.1016/j.dsr2.2018.05.006

Kozlowski W A, Deutschman D, Garibotti I, et al. 2011. An evaluation of the application of CHEMTAX to Antarctic coastal pigment data. Deep-Sea Research Part I: Oceanographic Research Papers, 58(4): 350–364, doi: 10.1016/j.dsr.2011.01.008

Landschützer P, Gruber N, Bakker D C E. 2016. Decadal variations and trends of the global ocean carbon sink. Global Biogeochemical Cycles, 30(10): 1396–1417, doi: 10.1002/2015gb005359

Lee Y, Yang E J, Park J, et al. 2016. Physical-biological coupling in the Amundsen Sea, Antarctica: influence of physical factors on phytoplankton community structure and biomass. Deep-Sea Research Part I: Oceanographic Research Papers, 117: 51–60, doi: 10.1016/j.dsr.2016.10.001

Loeb V, Hofmann E E, Klinck J M, et al. 2010. Hydrographic control of the marine ecosystem in the South Shetland-Elephant Island and Bransfield Strait region. Deep-Sea Research Part II: Topical Studies in Oceanography, 57(7–8): 519–542, doi: 10.1016/j.dsr2.2009.10.004

Lovenduski N S, Gruber N. 2005. Impact of the Southern Annular Mode on Southern Ocean circulation and biology. Geophysical Research Letters, 32(11): L11603, doi: 10.1029/2005gl022727

Martinson D G, Stammerjohn S E, Iannuzzi R A, et al. 2008. Western Antarctic Peninsula physical oceanography and spatio–tem-

poral variability. Deep-Sea Research Part II: Topical Studies in Oceanography, 55(18–19): 1964–1987, doi: 10.1016/j.dsr2.2008.04.038
McGillicuddy D J Jr, Sedwick P N, Dinniman M S, et al. 2015. Iron supply and demand in an Antarctic shelf ecosystem. Geophysical Research Letters, 42(19): 8088–8097, doi: 10.1002/2015GL065727
Mendes C R B, de Souza M S, Garcia V M T, et al. 2012. Dynamics of phytoplankton communities during late summer around the tip of the Antarctic Peninsula. Deep-Sea Research Part I: Oceanographic Research Papers, 65: 1–14, doi: 10.1016/j.dsr.2012.03.002
Mendes C R B, Tavano V M, Dotto T S, et al. 2018a. New insights on the dominance of cryptophytes in Antarctic coastal waters: a case study in Gerlache Strait. Deep-Sea Research Part II: Topical Studies in Oceanography, 149: 161–170, doi: 10.1016/j.dsr2.2017.02.010
Mendes C R B, Tavano V M, Kerr R, et al. 2018b. Impact of sea ice on the structure of phytoplankton communities in the northern Antarctic Peninsula. Deep-Sea Research Part II: Topical Studies in Oceanography, 149: 111–123, doi: 10.1016/j.dsr2.2017.12.003
Mendes C R B, Tavano V M, Leal M C, et al. 2013. Shifts in the dominance between diatoms and cryptophytes during three late summers in the Bransfield Strait (Antarctic Peninsula). Polar Biology, 36(4): 537–547, doi: 10.1007/s00300-012-1282-4
Moline M A, Claustre H, Frazer T K, et al. 2004. Alteration of the food web along the Antarctic Peninsula in response to a regional warming trend. Global Change Biology, 10(12): 1973–1980, doi: 10.1111/j.1365-2486.2004.00825.x
Montes-Hugo M, Doney S C, Ducklow H W, et al. 2009. Recent changes in phytoplankton communities associated with rapid regional climate change along the western Antarctic Peninsula. Science, 323(5920): 1470–1473, doi: 10.1126/science.1164533
Morel A, Huot Y, Gentili B, et al. 2007. Examining the consistency of products derived from various ocean color sensors in open ocean (Case 1) waters in the perspective of a multi-sensor approach. Remote Sensing of Environment, 111(1): 69–88, doi: 10.1016/j.rse.2007.03.012
Murphy E J, Watkins J L, Trathan P N, et al. 2007. Spatial and temporal operation of the Scotia Sea ecosystem: a review of large-scale links in a krill centred food web. Philosophical Transactions of the Royal Society B, 362(1477): 113–148, doi: 10.1098/rstb.2006.1957
Nunes S, Latasa M, Delgado M, et al. 2019. Phytoplankton community structure in contrasting ecosystems of the Southern Ocean: South Georgia, South Orkneys and western Antarctic Peninsula. Deep-Sea Research Part I: Oceanographic Research Papers, 151: 103059, doi: 10.1016/j.dsr.2019.06.005
Oksanen J, Blanchet F G, Kindt R, et al. 2013. Package 'vegan'. Community Ecology Package, 2(9): 1–295
Pallin L J, Baker C S, Steel D, et al. 2018. High pregnancy rates in humpback whales (*Megaptera novaeangliae*) around the western Antarctic Peninsula, evidence of a rapidly growing population. Royal Society Open Science, 5(5): 180017, doi: 10.1098/rsos.180017
Park J, Oh I S, Kim H C, et al. 2010. Variability of SeaWiFs chlorophyll-*a* in the southwest Atlantic sector of the Southern Ocean: strong topographic effects and weak seasonality. Deep-Sea Research Part I: Oceanographic Research Papers, 57(4): 604–620, doi: 10.1016/j.dsr.2010.01.004
Peck L S, Barnes D K A, Cook A J, et al. 2010. Negative feedback in the cold: ice retreat produces new carbon sinks in Antarctica. Global Change Biology, 16(9): 2614–2623, doi: 10.1111/j.1365-2486.2009.02071.x
Peeken I. 1997. Photosynthetic pigment fingerprints as indicators of phytoplankton biomass and development in different water masses of the Southern Ocean during austral spring. Deep-Sea Research Part II: Topical Studies in Oceanography, 44(1–2): 261–282, doi: 10.1016/s0967-0645(96)00077-x
Petrou K, Kranz S A, Trimborn S, et al. 2016. Southern Ocean phytoplankton physiology in a changing climate. Journal of Plant Physiology, 203: 135–150, doi: 10.1016/j.jplph.2016.05.004
Reiss C S, Hewes C D, Holm-Hansen O. 2009. Influence of atmospheric teleconnections and Upper Circumpolar Deep Water on phytoplankton biomass around Elephant Island, Antarctica. Marine Ecology Progress Series, 377: 51–62, doi: 10.3354/meps07840
Rodriguez F, Varela M, Zapata M. 2002. Phytoplankton assemblages in the Gerlache and Bransfield Straits (Antarctic Peninsula) determined by light microscopy and CHEMTAX analysis of HPLC pigment data. Deep-Sea Research Part II: Topical Studies in Oceanography, 49(4–5): 723–747, doi: 10.1016/S0967-0645(01)00121-7
Rozema P D, Venables H J, Van de Poll W H, et al. 2017. Interannual variability in phytoplankton biomass and species composition in northern Marguerite Bay (West Antarctic Peninsula) is governed by both winter sea ice cover and summer stratification. Limnology and Oceanography, 62(1): 235–252, doi: 10.1002/lno.10391
Russo A D P G, de Souza M S, Mendes C R B, et al. 2018. Spatial variability of photophysiology and primary production rates of the phytoplankton communities across the western Antarctic Peninsula in late summer 2013. Deep-Sea Research Part II: Topical Studies in Oceanography, 149: 99–1, doi: 10.1016/j.dsr2.2017.09.021
Sabine C L, Feely R A, Gruber N, et al. 2004. The oceanic sink for anthropogenic CO_2. Science, 305(5682): 367–371, doi: 10.1126/science.1097403
Sanchez N, Reiss C S, Holm-Hansen O, et al. 2019. Weddell-Scotia confluence effect on the iron distribution in waters surrounding the South Shetland (Antarctic Peninsula) and South Orkney (Scotia Sea) islands during the austral summer in 2007 and 2008. Frontiers in Marine Science, 6: 771, doi: 10.3389/fmars.2019.00771
Sangrà P, García-Muñoz C, García C M, et al. 2014. Coupling between upper ocean layer variability and size-fractionated phytoplankton in a non-nutrient-limited environment. Marine Ecology Progress Series, 499: 35–46, doi: 10.3354/meps10668
Sangrà P, Gordo C, Hernández-Arencibia M, et al. 2011. The Bransfield current system. Deep-Sea Research Part I: Oceanographic Research Papers, 58(4): 390–402, doi: 10.1016/j.dsr.2011.01.011
Schloss I R, Abele D, Moreau S, et al. 2012. Response of phytoplankton dynamics to 19-year (1991–2009) climate trends in Potter Cove (Antarctica). Journal of Marine Systems, 92(1): 53–66, doi: 10.1016/j.jmarsys.2011.10.006
Secchi E R, Dalla-Rosa L, Kinas P G, et al. 2011. Encounter rates and abundance of humpback whales (*Megaptera novaeangliae*) in Gerlache and Bransfield Straits, Antarctic Peninsula. Journal of Cetacean Research and Management, 3: 107–111, doi: 10.47536/jcrm.vi.312
Seyboth E, Botta S, Mendes C R B, et al. 2018. Isotopic evidence of the effect of warming on the northern Antarctic Peninsula ecosystem. Deep-Sea Research Part II: Topical Studies in Oceanography, 149: 218–228, doi: 10.1016/j.dsr2.2017.12.020
Shepherd A, Ivins E, Rignot E, et al. 2018. Mass balance of the Antarctic Ice Sheet from 1992 to 2017. Nature, 558(7709): 219–222, doi: 10.1038/s41586-018-0179-y
Stammerjohn S E, Martinson D G, Smith R C, et al. 2008. Trends in Antarctic annual sea ice retreat and advance and their relation to El Niño–Southern Oscillation and Southern Annular Mode variability. Journal of Geophysical Research: Oceans, 113(C3): C03S90, doi: 10.1029/2007jc004269
Steig E J, Schneider D P, Rutherford S D, et al. 2009. Warming of the Antarctic ice-sheet surface since the 1957 International Geophysical Year. Nature, 457(7228): 459–462, doi: 10.1038/nature07669
Takahashi T, Sutherland S C, Sweeney C, et al. 2002. Global sea–air CO_2 flux based on climatological surface ocean pCO_2, and seasonal biological and temperature effects. Deep-Sea Research Part II: Topical Studies in Oceanography, 49(9–10): 1601–1622, doi: 10.1016/S0967-0645(02)00003-6

Thompson A F, Heywood K J, Thorpe S E, et al. 2009. Surface circulation at the tip of the Antarctic peninsula from drifters. Journal of Physical Oceanography, 39(1): 3–26, doi: 10.1175/2008jpo3995.1

Tréguer P, Bowler C, Moriceau B, et al. 2018. Influence of diatom diversity on the ocean biological carbon pump. Nature Geoscience, 11(1): 27–37, doi: 10.1038/s41561-017-0028-x

Turner J, Phillips T, Marshall G J, et al. 2017. Unprecedented springtime retreat of Antarctic sea ice in 2016. Geophysical Research Letters, 44(13): 6868–6875, doi: 10.1002/2017gl073656

Van de Poll W H, Lagunas M, de Vries T, et al. 2011. Non-photochemical quenching of chlorophyll fluorescence and xanthophyll cycle responses after excess PAR and UVR in *Chaetoceros brevis, Phaeocystis antarctica* and coastal Antarctic phytoplankton. Marine Ecology Progress Series, 426: 119–131, doi: 10.3354/meps09000

Villafañe V E, Janknegt P J, de Graaff M, et al. 2008. UVR-induced photoinhibition of summer marine phytoplankton communities from Patagonia. Marine Biology, 154(6): 1021–1029, doi: 10.1007/s00227-008-0993-0

Von Gyldenfeldt A B, Fahrbach E, García M A, et al. 2002. Flow variability at the tip of the Antarctic Peninsula. Deep-Sea Research Part II: Topical Studies in Oceanography, 49(21): 4743–4766, doi: 10.1016/S0967-0645(02)00157-1

Wang Bo, Chen Min, Chen Feng, et al. 2020. Meteoric water promotes phytoplankton carbon fixation and iron uptake off the eastern tip of the Antarctic Peninsula (eAP). Progress in Oceanography, 185: 102347, doi: 10.1016/j.pocean.2020.102347

Westwood K J, Griffiths F B, Meiners K M, et al. 2010. Primary productivity off the Antarctic coast from 30°–80°E; BROKE-West survey, 2006. Deep-Sea Research Part II: Topical Studies in Oceanography, 57(9–10): 794–814, doi: 10.1016/j.dsr2.2008.08.020

Wojtasiewicz B, Trull T W, Clementson L, et al. 2019. Factors controlling the lack of phytoplankton biomass in naturally iron fertilized waters near heard and McDonald islands in the Southern Ocean. Frontiers in Marine Science, 6: 531, doi: 10.3389/fmars.2019.00531

Wright S W, Ishikawa A, Marchant H J, et al. 2009. Composition and significance of picophytoplankton in Antarctic waters. Polar Biology, 32(5): 797–808, doi: 10.1007/s00300-009-0582-9

Zapata M, Rodríguez F, Garrido J. 2000. Separation of chlorophylls and carotenoids from marine phytoplankton: a new HPLC method using a reversed phase C8 column and pyridine-containing mobile phases. Marine Ecology Progress, 195(3): 29-45. https://doi.org/10.3354/meps195029

Zhang Run, Ma Qiang, Chen Min, et al. 2019. Nitrogen uptake regime regulated by ice melting during austral summer in the Prydz Bay, Antarctica. Acta Oceanologica Sinica, 38(8): 1–7, doi: 10.1007/s13131-019-1434-2

Zhang Run, Zheng Minfang, Chen Min, et al. 2014. An isotopic perspective on the correlation of surface ocean carbon dynamics and sea ice melting in Prydz Bay (Antarctica) during austral summer. Deep-Sea Research Part I: Oceanographic Research Papers, 83: 24–33, doi: 10.1016/j.dsr.2013.08.006

Zhuang Yanpei, Jin Haiyan, Li Hongliang, et al. 2014. Phytoplankton composition and its ecological effect in subsurface cold pool of the northern Bering Sea in summer as revealed by HPLC derived pigment signatures. Acta Oceanologica Sinica, 33(6): 103–111, doi: 10.1007/s13131-014-0495-5

Supplementary information:

Fig. S1. Detailed retention time and chromatogram of pigments (used pigments in red font) measured by UPLC. a. mixed standards-a; b. mixed standards-b.

Fig. S2. Distribution of temperature (a) and salinity (b) across the water column (i.e., 0 m, 25 m, 50 m, 100 m, 200 m).

Fig. S3. Distribution of nitrate concentration (a), phosphate concentration (b) and silicate concentration (c) across the water column (i.e., 0 m, 25 m, 50 m, 100 m, 200 m).

Fig. S4. Distribution of N/P ratios (a), Si/P ratios (b) and N/Si ratios (c) across the water column (i.e., 0 m, 25 m, 50 m, 100 m, 200 m, respectively).

Fig. S5. Distribution of chlorophyll *a* (a), pheophorbide *a* (b), pheophytin *a* (c), fucoxanthin (d), chlorophyll c_2 (e), chlorophyll c_3 (f), and chlorophyll *b* (g) concentrations in the water column (i.e., 0 m, 25 m, 50 m, 100 m, 200 m, respectively).

Fig. S6. The distributions of temperature (a), salinity (b), the percentage of diatoms (c) and *P. antarctica* (d) in Section L1. The location of Section L1 is shown in Plot b.

Fig. S7. The distributions of temperature (a), salinity (b), the percentage of diatoms (c) and *P. antarctica* (d) in Section L2. The location of Section L2 is shown in Plot b.

Table S1. The ratio of the two mobile phases varies with time in the Ultra Performance Liquid Chromatography (UPLC) binary gradient elution program, according to the method of Zapata et al. (2000).

Table S2. The abbreviation and retention time of the pigment measured by UPLC.

Table S3. The percentage of different phytoplankton taxonomic groups in the water column.

Table S4. Correlations of the mean value of studying parameters at all study sites. Only data with significant correlations at the 0.05 level are shown, the underlined number is significant at the 0.01 level.

Table S5. Phytoplankton taxonomic composition (relative abundance) in the surface layer of the study area based on CHEMTAX calculation.

The supplementary information is available online at https://doi.org/10.1007/s13131-021-1865-4 and www.aosocean.com. The supplementary information is published as submitted, without typesetting or editing. The responsibility for scientific accuracy and content remains entirely with the authors.